

Ultrafast Excitonic and Charge Transfer Dynamics in Nanostructured Organic Polymer Materials

I. Burghardt[†], P. Eisenbrandt[†], M. Polkehn[†], S. Haacke[‡], S. Méry[‡], H. Tamura⁺

[†]Institute for Physical and Theoretical Chemistry, Goethe University Frankfurt, Germany

[‡]Institut de Physique et Chimie des Matériaux de Strasbourg, Université de Strasbourg, France

⁺Advanced Institute for Materials Research, University of Tohoku, Sendai, Japan

Nanophotonics – Conference 9884

Session 6: Control of Nanoscale Optical and Electronic Processes

[SPIE Photonics Europe](#)

Bruxelles, 5 April 2016

Topics

- 1 Photoinduced Energy & Charge Transfer in Functional Organic Materials
Goal: First-Principles Approach to Organic Photovoltaics
Electron-Hole Lattice Models & Electron-Phonon Coupling
Quantum Dynamics in Many Dimensions

Topics

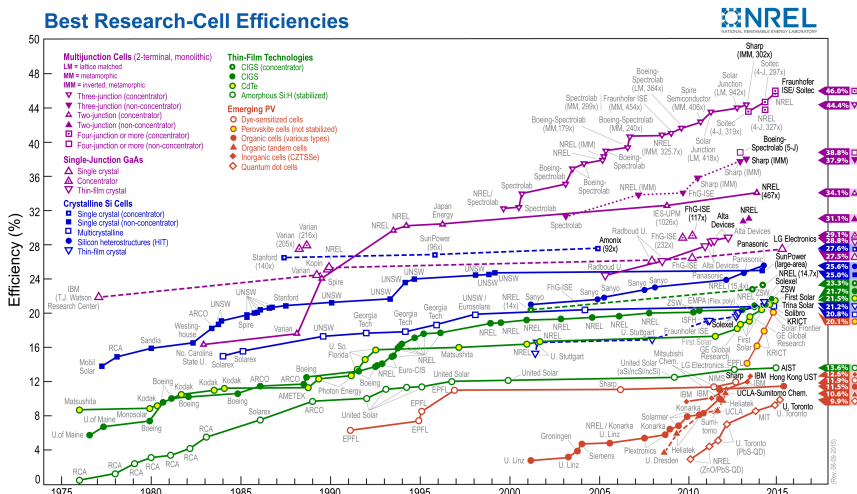
- ① Photoinduced Energy & Charge Transfer in Functional Organic Materials
Goal: First-Principles Approach to Organic Photovoltaics
Electron-Hole Lattice Models & Electron-Phonon Coupling
Quantum Dynamics in Many Dimensions
- ② Case Studies I: Charge Separation in Organic Photovoltaics
Oligothiophene-Fullerene (P3HT:PCBM Type) Junctions
Highly Ordered Oligothiophene-Perylene Assemblies
Charge Transfer Excitons in Neat Polythiophene

Topics

- ① Photoinduced Energy & Charge Transfer in Functional Organic Materials
Goal: First-Principles Approach to Organic Photovoltaics
Electron-Hole Lattice Models & Electron-Phonon Coupling
Quantum Dynamics in Many Dimensions
- ② Case Studies I: Charge Separation in Organic Photovoltaics
Oligothiophene-Fullerene (P3HT:PCBM Type) Junctions
Highly Ordered Oligothiophene-Perylene Assemblies
Charge Transfer Excitons in Neat Polythiophene
- ③ Case Studies II: Singlet Exciton Fission, Exciton Migration
Singlet Exciton Fission: Pentacene and Rubrene
Exciton Transport across Geometric Defects: Torsion-Induced EET
Summary & Outlook

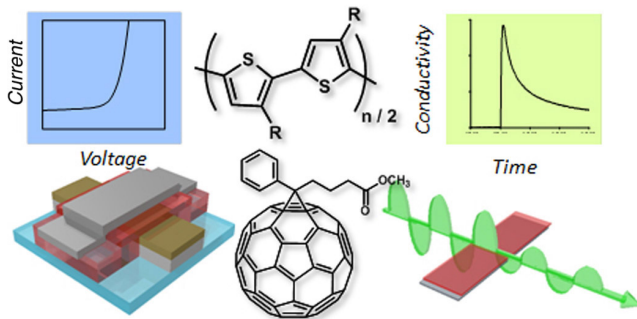
OPV: Not Yet Competitive ... But Making Progress!

Best Research-Cell Efficiencies



<http://www.nrel.gov/ncpv/> (National Center for Photovoltaics)

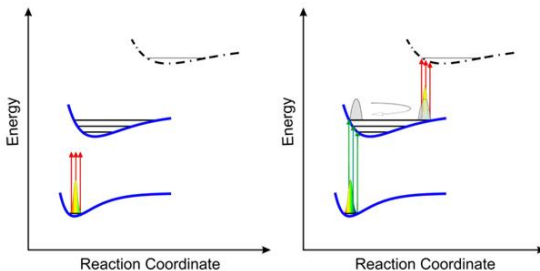
How to Optimize Devices: Synthesis/Spectroscopy/Theory



A speedier way to evaluate organic photovoltaics, Akinori Saeki, SPIE Newsroom. DOI: 10.1117/2.1201111.003967

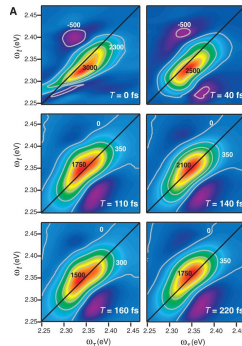
- **synthetic chemistry:** optimized donor-acceptor combinations
- **spectroscopy:** optical spectroscopy, time-resolved microwave conductivity, terahertz time-domain spectroscopy, electroabsorption spectroscopy, ...
- **theoretical chemistry:** electronic structure + quantum dynamics

Nonlinear Optical Spectroscopy



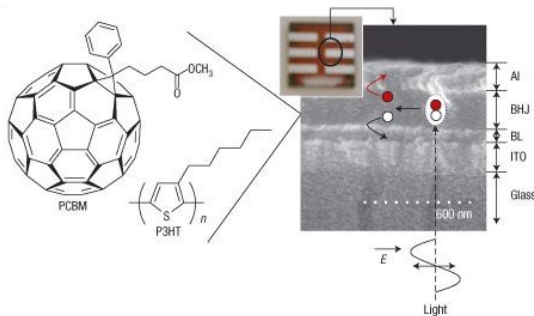
<http://www.uni-heidelberg.de/fakultaeten/chemgeo/pci/motzkus/research/wavepackets.html>

- time-resolved photoluminescence
- **pump-probe** spectroscopy: e.g., transient absorption
- **2D electronic spectroscopy**: photon echo type measurements
- monitor molecular excited-state populations and coherences
- semiclassical treatment of matter-field interaction



Collini, Scholes, Science 323, 369 (2009)

Elementary Processes of Organic Photovoltaics



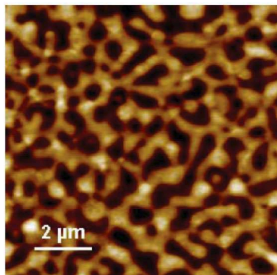
Kim et al., Nature Materials, 5, 197 (2006)

elementary steps:

- creation of electron-hole pairs (excitons)
- exciton dissociation at donor-acceptor junctions (here, PCBM-P3HT)¹
- capture of charge carriers at electrodes
- potentially competing process: electron-hole recombination

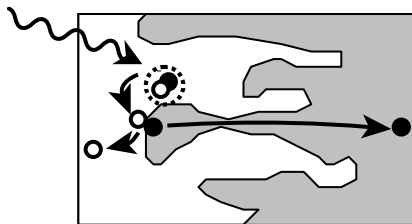
¹PCBM = phenyl-C₆₁-butyric acid methyl ester, P3HT = poly(3-hexylthiophene)

Bulk Heterojunctions (BHJ's)



AFM image of d-F8:F8BT blend

McNeill & Greenham, Adv. Mater. 21, 1 (2009)



Schematic of exciton dissociation

Peumans, Uchida, Forrest, Nature **125**, 8098 (2003)

- so-called **bulk heterojunction** technology led to breakthrough in ~ 1995
- maximization of interface area \rightarrow increase likelihood that excitons encounter interface within diffusion length ~ 10 nm

What is the Best Nano-Morphology?

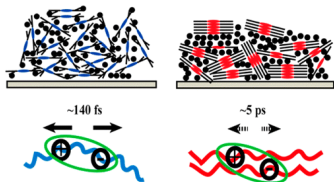
Highly ordered nanostructured domains (typically sub-10 nm) are thought to

- facilitate exciton diffusion
- favor exciton dissociation
- facilitate free carrier transport

Nanostructured domains can be achieved by

- self-assembly properties of D/A oligomers
- thin film processing methods (e.g., nanoimprint lithography)

However, the role of nanoscale ordering is controversial:

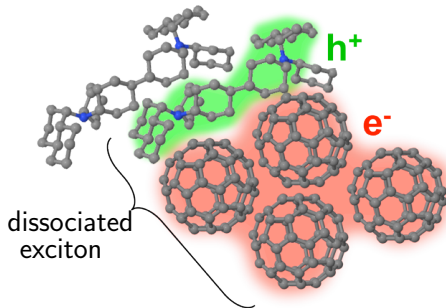


Guo et al., JACS 136, 10024 (2014)

- e.g., in a recent study of DA copolymer:fullerene systems, it is shown that the charge separation energetics changes **unfavorably** upon formation of crystalline domains

Which Methods, Even for a Minimal Model?

- tens to hundreds of electronic states
- aggregate-type systems
- charge transfer and excitonic couplings^(*) required
- delocalized excitations
- strong electron-phonon coupling
- non-Markovian dynamics
- non-exponential transfer
- coherent wavepacket dynamics
- standard rate theories (Förster / Marcus) not necessarily valid



<http://phys.org/news/2014-02-result-cheaper-efficient-solar-cells.html>

^(*)excitonic coupling = transition density interaction:

$$V_{DA} = \frac{1}{4\pi\epsilon_0} \int d\mathbf{r}_D d\mathbf{r}_A \frac{\rho_D^{(eg)}(\mathbf{r}_D) \rho_A^{(ge)}(\mathbf{r}_A)}{|\mathbf{r}_D - \mathbf{r}_A|} \longrightarrow \text{limiting case: transition dipole interaction}$$

Two Types of Approaches

approximate electron-nuclear dynamics:
 time-dependent Kohn-Sham equation

$$i\frac{\partial}{\partial t}\phi_i(r,t) = \left(-\frac{\nabla^2}{2} + v_{\text{KS}}(r,t)\right)\phi_i(r,t)$$

expand in adiabatic KS basis,
 $\phi_i(r,t) = \sum_k c_{ik}(t)\tilde{\phi}_k(r;R)$ such that

$$i\frac{dc_{ik}}{dt} = \sum_l c_{il}(t)(\epsilon_l\delta_{kl} + d_{kl}\cdot\dot{R})$$

Ehrenfest or Surface Hopping dynamics

e.g., Craig, Duncan, Prezhd, PRL 95, 163001 (2005)

pro's: no pre-computed potentials
con's: possibly poor description of excited
 states and nuclear dynamics

parametrized model Hamiltonian
 + multi-state quantum nuclear dynamics

$$i\frac{\partial}{\partial t}\psi(R,t) = \hat{H}\psi(R,t)$$

with a multi-state/site Hamiltonian

$$\hat{H} = \sum_{mn}(\hat{h}_{mn}^e + \hat{h}_{mn}^{e-ph}(R))|m\rangle\langle n| + \hat{H}_0^{ph}(R)$$

and $|\psi(R,t)\rangle = \sum_n c_n(t)\Phi_n(R,t)|n\rangle$

use (approximate) quantum dynamics

e.g., Kondov et al., JPCC 111 (2007), Tamura et al., JACS 135 (2013)

pro's: immediate physical interpretation
con's: restricted number of coordinates,
 electronic couplings *via* diabaticization

Road Map: Model Hamiltonians & Quantum Dynamics

e-h lattice models + non-perturbative *e-ph* interaction + quantum dynamics

- electron-hole (*e-h*) lattice models including vibronic interactions
- *ab initio* (typically CC2, ADC(2)) or TD-DFT parametrization; diabaticization procedures to generate electronic couplings
- compute spectral densities and effective-mode decomposition
- efficient high-dimensional nonadiabatic quantum dynamics using multi-configurational methods (MCTDH) or reduced dynamics (HEOM)

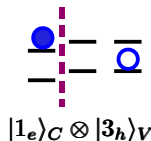
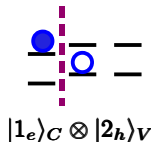
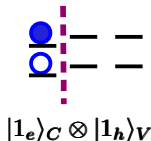
CC2 = Second-Order Approximate Coupled-Cluster

ADC(2) = Second-Order Algebraic-Diagrammatic Construction (ADC(2)) scheme

MCTDH = Multi-Configuration Time-Dependent Hartree Beck et al., Phys. Rep. **324**, 1 (2000)

HEOM = Hierarchy of Equations of Motion Tanimura, J. Phys. Soc. Jpn. **75**, 082001 (2006)

Electron-Hole Lattice Model



- electron-hole ($e-h$) configurations:

$$|\mathbf{n}\rangle = |n_e n'_h\rangle = |n_e\rangle_C \otimes |n'_h\rangle_V$$

- Hamiltonian in this basis:

$$\hat{H} = \sum_{\mathbf{m}\mathbf{n}} (\hat{h}_{\mathbf{m}\mathbf{n}}^{eh} + \hat{h}_{\mathbf{m}\mathbf{n}}^{eh-ph}(\mathbf{x})) |\mathbf{m}\rangle \langle \mathbf{n}| + \hat{H}_0^{ph}(\mathbf{x})$$

Merrifield, J. Chem. Phys. 34, 1835 (1961)

Wang and Mukamel, Chem. Phys. Lett. 192, 417 (1992)

Karabunarliev and Bittner, J. Chem. Phys. 118, 4291 (2003)

Binder, Wahl, Römer, Burghardt, Faraday Discuss, 163, 205 (2013)

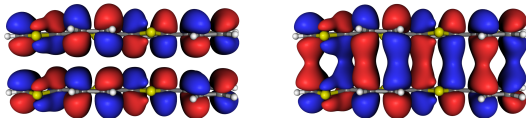
- includes Frenkel-type exciton (XT) states and charge transfer (CT) states
- oligomer (fragment) *ab initio* calculations:
obtain diabatic couplings & vibronic couplings
- NB: we don't use the Tamm-Dancoff approximation (TDA) which has shortcomings in describing excitons in organic semiconductors

Grüning, Marini, Gonze, Nano Lett. 9, 2820 (2009)

Special Case: Frenkel Exciton Model

- Frenkel model ($n_e = n'_h$) often a good approximation to describe exciton
- exact analytic mapping of oligomer PES's to Frenkel model

Binder, Römer, Wahl, Burghardt, J. Chem. Phys. 141, 014101 (2014)



stacked oligothiophene (OT4)₂: “HJ aggregate”

- delocalized states

$$|\Psi_{\text{exciton}}\rangle = \sum_n^{n_{\text{exc}}} c_n |\Phi_n\rangle$$

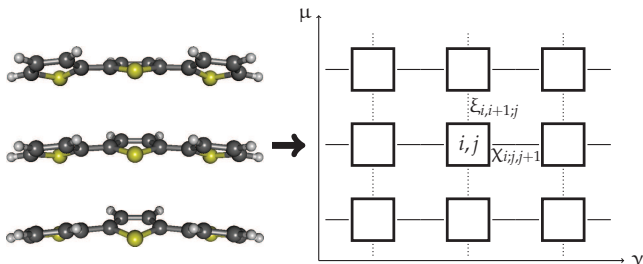
where $n_{\text{exc}} \sim 5-10$; $|\Phi_n\rangle =$ configuration with single excitation on n th monomer

- trapping due to exciton-phonon interactions

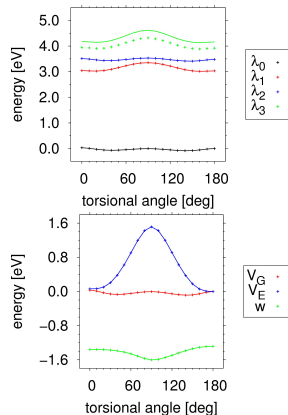
- **J-aggregate**: end-to-end alignment of monomer units; lowest state of the exciton manifold is the bright state
- **H-aggregate**: plane-to-plane stacked geometry; highest state of the exciton manifold is the bright state
- **HJ-aggregate**: combination of both, as in stacked oligomers

Yamagata, Spano, JCP 136, 184901 (2012)

HJ-Aggregate: Vibronic Lattice Model

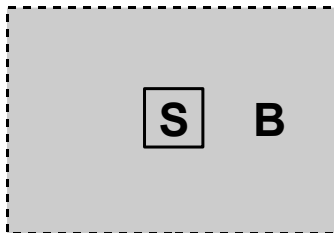
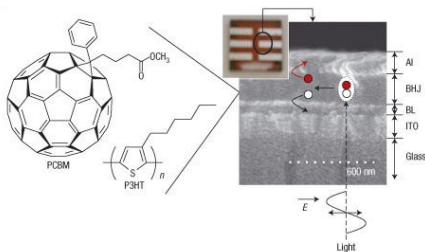


Binder, Römer, Wahl, Burghardt, J. Chem. Phys. 141, 014101 (2014)



- analytic mapping of oligomer PES onto Hückel type model (1D or 2D)
(NB.: V_G/V_E : monomer potentials, w : site-to-site coupling)

System-Bath Models



S region: e.g., electronic degrees of freedom (electron-hole states)

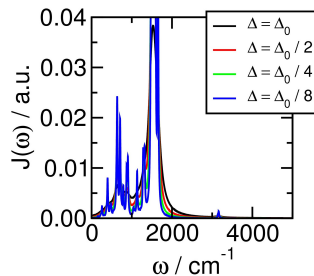
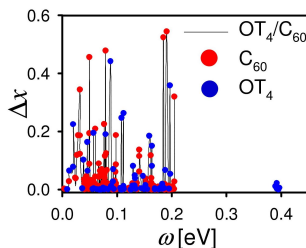
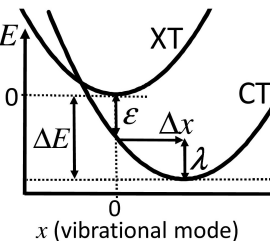
B region: all vibrations (phonons) mapped to harmonic oscillator model

$$\hat{H}_B + \hat{H}_{SB} = \sum_n \frac{1}{2} (\hat{p}_n^2 + \frac{1}{2} \omega_n^2 \hat{x}_n^2) + \hat{s} \sum_n c_n \hat{x}_n$$

$$J(\omega) = \pi/2 \sum_n c_n^2 / \omega_n \delta(\omega - \omega_n)$$

spectral density

Spectral Densities from Electronic Structure Calculations^(*)



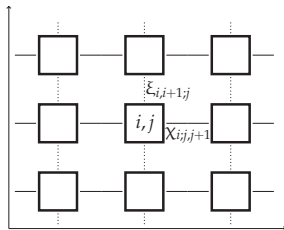
$$J(\omega) = \frac{\pi}{2} \sum_n \frac{c_n^2}{\omega_n} \delta(\omega - \omega_n) \simeq \frac{\pi}{2} \sum_n \frac{c_n^2}{\pi} \frac{\Delta}{(\omega - \omega_n)^2 + \Delta^2}$$

Tamura, Martinazzo, Ruckebauer, Burghardt, J. Chem. Phys., 137, 22A540 (2012)

^(*)NB. Alternatively: obtain SD's from correlation functions (MD, CPMD, ...)

Generalized Spin-Boson Models

$$\hat{H} = \hat{H}_S + \hat{H}_{SB} + \hat{H}_B = \sum_{\mathbf{mn}} \left(\hat{h}_{\mathbf{mn}}^{eh} + \sum_i c_i^{\mathbf{nm}} f(\hat{x}_i) \right) |\mathbf{n}\rangle \langle \mathbf{m}| + \sum_i \frac{\omega_i}{2} (\hat{p}_i^2 + \hat{x}_i^2)$$



- coupling through one or several subsystem operators $\hat{s} = |\mathbf{n}\rangle \langle \mathbf{m}|$ where $|\mathbf{n}\rangle = |n_e n'_h\rangle$
- system-bath couplings generally determined from **spectral densities**
 $J(\omega) = \pi/2 \sum_i c_i^2 / \omega_i \delta(\omega - \omega_i)$
- bath operators \hat{x}_i can couple in a **correlated** fashion to subsystem operators
- important (anharmonic) bath modes can be absorbed into the system part

Unitary Propagation vs. Master Equations

- ① explicit, multidimensional dynamics for the full system + bath space:
wavefunction $\psi_{SB}(t)$ or density operator $\hat{\rho}_{SB}(t) = \sum_n p_n |\psi_{n,SB}(t)\rangle \langle \psi_{n,SB}(t)|$
→ typically **MCTDH**
Meyer, Manthe, Cederbaum, Chem. Phys. Lett. **165**, 73 (1990), Beck et al., Phys. Rep. **324**, 1 (2000)
- ② reduced dynamics (master equation) methods: $\hat{\rho}_S(t) = \text{Tr}_B \hat{\rho}_{SB}(t)$
→ typically **Hierarchy of Equations of Motion (HEOM)**
Tanimura, J. Phys. Soc. Jpn. **75**, 082001 (2006)
- ③ intermediate methods: explicit treatment of **subsystem + effective-mode (E) part of the bath** + master equation for residual (B') bath:²

$$\frac{\partial \hat{\rho}_{SE}}{\partial t} = -\frac{i}{\hbar} [\hat{H}_{SE}, \hat{\rho}_{SE}(t)] + \hat{L}_{\text{diss}}^{(B')} \hat{\rho}_{SE}(t) \quad ; \quad \hat{\rho}_{SE}(t) = \text{Tr}_{B'} \hat{\rho}_{SEB'}(t)$$

²e.g., Caldeira-Leggett: $\hat{L}_{\text{diss}}^{(B')} \hat{\rho}_{SE} = -i \frac{\gamma}{\hbar} [\hat{X}_E, [\hat{P}_E, \hat{\rho}_{SE}]_+] - \frac{2\gamma M k T}{\hbar^2} [\hat{X}_E, [\hat{X}_E, \hat{\rho}_{SE}]]$

Unitary System + Bath Dynamics: MCTDH

$$\Psi(r, t) = \sum_J A_J(t) \Phi_J(r, t) \equiv \sum_{j_1=1}^{n_1} \dots \sum_{j_N=1}^{n_N} A_{j_1 \dots j_N}(t) \varphi_{j_1}^{(1)}(r_1, t) \dots \varphi_{j_N}^{(N)}(r_N, t)$$

- **Multi-Configuration Time-Dependent Hartree**: tensor approximation scheme
Meyer, Manthe, Cederbaum, Chem. Phys. Lett. **165**, 73 (1990), Beck et al., Phys. Rep. **324**, 1 (2000)
- EoM's from the Dirac-Frenkel variational principle: $\langle \delta \Psi | \hat{H} - i \frac{\partial}{\partial t} | \Psi \rangle = 0$
- MCTDH takes one to **50-100 modes**; exponential scaling alleviated
- restriction on the form of the potential: sums over products
- related multi-layer variant (**ML-MCTDH**) goes up to **1000 modes**
Wang, Thoss, J. Chem. Phys. **119**, 1289 (2003)
- related **MCTDH-F** (fermion) and **MCTDH-B** (boson) methods
Kato, Kono, Chem. Phys. Lett. **392**, 533 (2004), Nest, Klamroth, Saalfrank, J. Chem. Phys. **122**, 124102 (2005)
Alon, Streltsov, Cederbaum, Phys. Lett. A **362**, 453 (2007)
- **density matrix** variant
Raab, Burghardt, Meyer, J. Chem. Phys. **111**, 8759 (1999)
- **hybrid** approaches: e.g., Gaussian-based variant (**G-MCTDH**, **vMCG**)
Burghardt, Meyer, Cederbaum, J. Chem. Phys. **111**, 2927 (1999), Worth, Burghardt, Chem. Phys. Lett. **368**, 502 (2003)

Non-Markovian Reduced Dynamics: HEOM

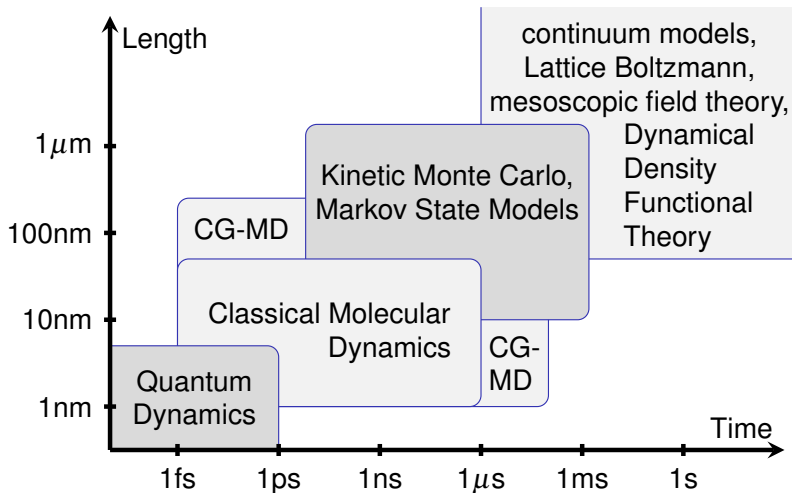
(collaboration K. H. Hughes (Bangor University, UK))

Tanimura, J. Phys. Soc. Jpn. **75**, 082001 (2006), Hughes, Cahier, Martinazzo, Burghardt, Chem. Phys., 442, 111 (2014)

$$\begin{aligned} \frac{\partial \hat{\rho}_{\mathbf{n}}}{\partial t} = & (-i\hat{\mathcal{L}}_S + \sum_{k=1}^N n_k h_k) \hat{\rho}_{\mathbf{n}} - i \sum_{k=1}^N [\hat{s}, \hat{\rho}_{\mathbf{n}^+}] \\ & - i \sum_{k=1}^N g_k n_k [\hat{s}, \hat{\rho}_{\mathbf{n}^-}] - \sum_{k=1}^{2M} f_k n_k [\hat{s}, \hat{\rho}_{\mathbf{n}^-}] + \end{aligned}$$

- **HEOM = Hierarchical Equations of Motion** Tanimura, J. Phys. Soc. Jpn. **75**, 082001 (2006)
- general n th-level auxiliary density operators (ADO) $\hat{\rho}_{\mathbf{n}}$
- \mathbf{n} is integer array with n_{exp} entries (from multi-exp. decomposition of $\mathcal{C}_B(t)$)
- correlation functions: $\mathcal{C}_B(t) = \sum_l g_l \exp(h_l t) - i \sum_l f_l \exp(h_l t)$
- \mathbf{n}^+ and \mathbf{n}^- generate hierarchy up/down-coupling
- Time Non-Local (TNL) closure (setting all ADOs to zero for $n_H + 1$ level)
- e.g., $n = 10$, $M = 5$, hence $(n_{\text{exp}} + n)! / (n!(n_{\text{exp}} - 1)!) = 1,847,560$ ADOs

Hierarchy of Time and Length Scales



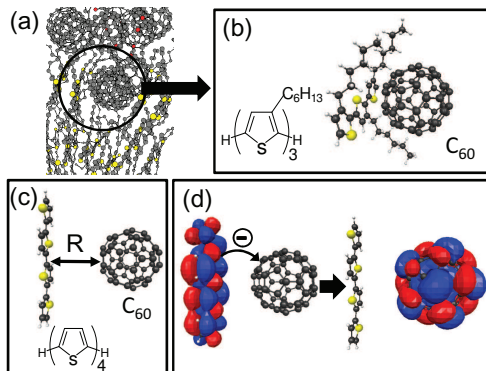
- *e-h* model Hamiltonians carry over, e.g., to Kinetic Monte Carlo framework

Topics

- ① Photoinduced Energy & Charge Transfer in Functional Organic Materials
Goal: First-Principles Approach to Organic Photovoltaics
Electron-Hole Lattice Models & Electron-Phonon Coupling
Quantum Dynamics in Many Dimensions
- ② **Case Studies I: Charge Separation in Organic Photovoltaics**
Oligothiophene-Fullerene (P3HT:PCBM Type) Junctions
Highly Ordered Oligothiophene-Perylene Assemblies
Charge Transfer Excitons in Neat Polythiophene
- ③ Case Studies II: Singlet Exciton Fission, Exciton Migration
Singlet Exciton Fission: Pentacene and Rubrene
Exciton Transport across Geometric Defects: Torsion-Induced EET
Summary & Outlook

Oligothiophene-Fullerene Junctions

(collaboration with Hiroyuki Tamura (Sendai), Keith Hughes (Bangor), Rocco Martinazzo (Milano))

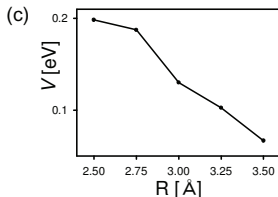
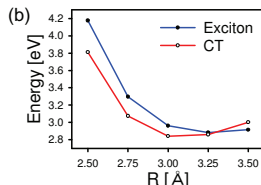
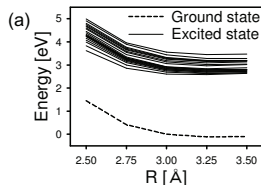


Tamura, Burghardt, Tsukada, JPCC, **115**, 10205 (2011)

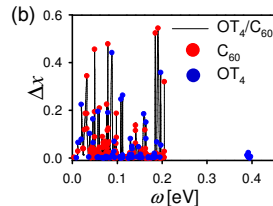
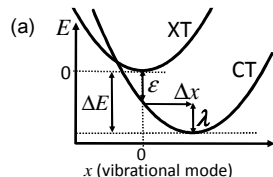
- model for polymer-fullerene heterojunctions, e.g., P3HT-PCBM ¹
- ultrafast initial charge transfer (~ 50 fs [Brabec et al., CPL (2001)])
- but subsequent generation of free charge carriers not necessarily ultrafast

¹PCBM = phenyl-C₆₁-butyric acid methyl ester, P3HT = poly(3-hexylthiophene)

Oligothiophene-Fullerene Junction: Dimer Model



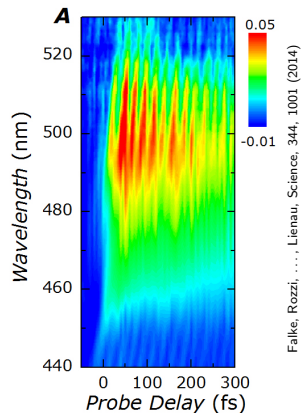
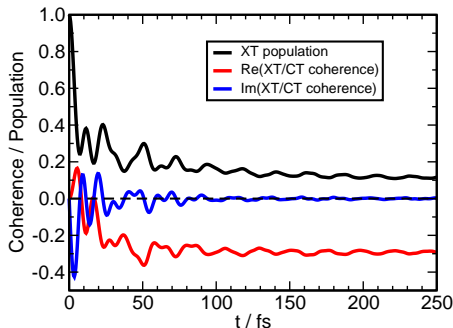
diabatic coupling:
distance dependence



- LC-TDDFT calculations (LC = long-range corrected)
- diabaticization scheme using reference functions of pure XT vs. CT character
- normal mode analysis for separate C_{60}^- and OT_4^+ fragments (264 modes)

Tamura, Burghardt, Tsukada, J. Phys. Chem. C, 115, 10205 (2011)

Ultrafast Coherent Transfer Dynamics

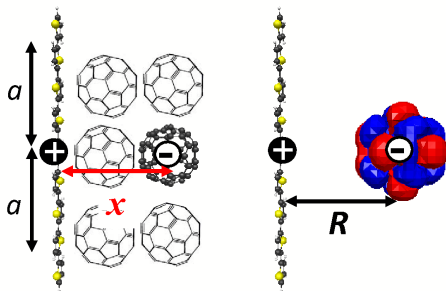


el. coherence: $\rho_{XT,CT}(t) = \text{Tr}\{ |CT\rangle \langle XT| \hat{\rho}(t) \}$

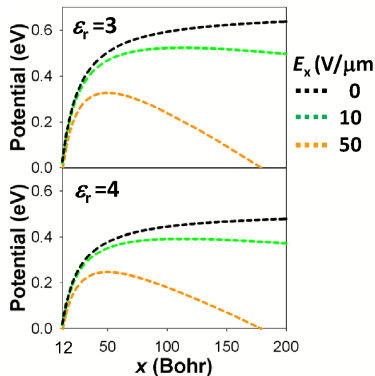
- imaginary part $(-2\gamma/\hbar)\text{Im}\rho_{XT,CT} \leftrightarrow$ population flux
- real part \leftrightarrow stationary coherent superposition ($P_{XT} \sim 0.1$, $P_{CT} \sim 0.9$)
- **experiment:** ultrafast ET (~ 50 fs), oscillatory features [Brabec et al., CPL (2001)] confirmed by recent pump-probe experiments by Lienau group [Science (2014)]

Free Carrier Generation

(collaboration with Hiroyuki Tamura (WPI-AIMR Tohoku University))



Tamura, Burghardt, JPCC, 117, 15020 (2013)



- Coulomb barrier to free carrier generation
- validity of Onsager-Braun rate model for CT break-up to be questioned
- “hot CT” hypothesis: efficient charge separation due to excess energy
- time scale of free carrier generation controversial & system-dependent (fs-μs)

Electron Delocalization in Ordered Fullerene Domains is Crucial

- significant reduction of barrier height as a function of fullerene aggregation
- in agreement with recent experiments

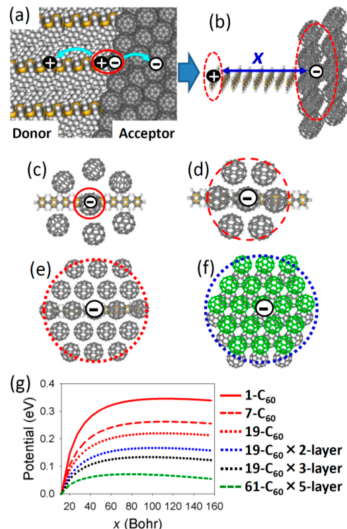
Gélinas et al., Scienceexpress 10.1126/science.1246249

Electro-Absorption (EA) experiments detect charge separated species

EA signal only observed for high fullerene loading, e.g., 1:4 D/A mixture, **not** for 4:1 mixture^(*)

ultrafast charge separation of ~ 5 nm, impeding recombination

^(*) However, **both** blends exhibit < 100 fs XT quenching



Tamura, Burghardt, JACS (Communication) 135, 16364 (2013)

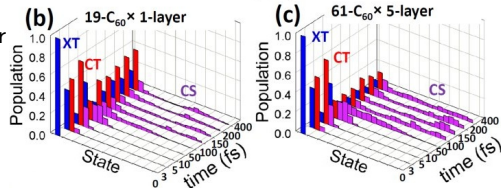
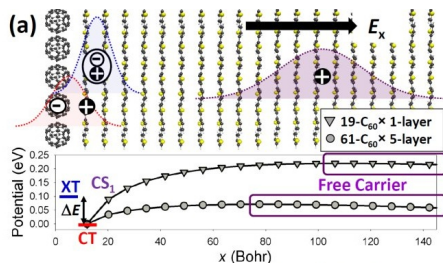
Dynamics of Free Carrier Generation

$$\hat{H} = \hat{H}_{\text{XT-CT}}(\mathbf{x}) + \sum_n \hat{H}_{\text{CS}}^{(n)}(\mathbf{x}) |\text{CS}_n\rangle \langle \text{CS}_n| + t(\mathbf{x}) (|\text{CS}_1\rangle \langle \text{CT}| + \sum_{nn'} |\text{CS}_n\rangle \langle \text{CS}_{n'}| + h.c.)$$

- extended XT/CT/CS Hamiltonian
- MCTDH calculations
(20 states, 110 modes)
- transfer integrals: $t \sim 0.1$ eV

factors favoring ultrafast e - h separation:

- exciton (XT) excess energy:
“Hot CT” mechanism
- XT delocalization in H-aggregate donor
- hole delocalization due to oligomer
(thiophene) conjugation
- electron delocalization over fullerene
aggregates: strong decrease of barrier



Tamura, Burghardt, JACS (Communication) 135, 16364 (2013)

“Quantum coherence controls the charge separation in a prototypical organic photovoltaic system”

Lienau and collaborators (Science, 2014)

We subscribe to this, in the following sense:

- the primary processes are determined by **coherent dynamics**
- time-dependent off-diagonal density matrix elements in the eigenstate basis
- equivalently: vibronic wavepacket motion → **can't use Marcus theory!**

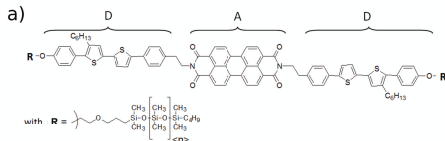
- another aspect: **spatial coherence** (e.g., exciton “coherence size”)
- this is closely connected to a site-local basis
- quasi-stationary spatially coherent states: e.g., trapped Frenkel states

- for now: disregard issue of coherent/incoherent light sources (cf. P. Brumer)

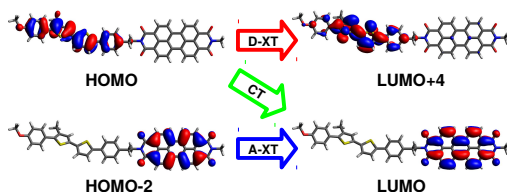
- we note that at longer times, most processes can be captured by kinetic equations: e - h recombination, charge carrier transport and trapping, etc.

Highly Ordered DA Assemblies: First-Generation LC Material

collaboration with S. Haacke, S. Méry (Strasbourg)



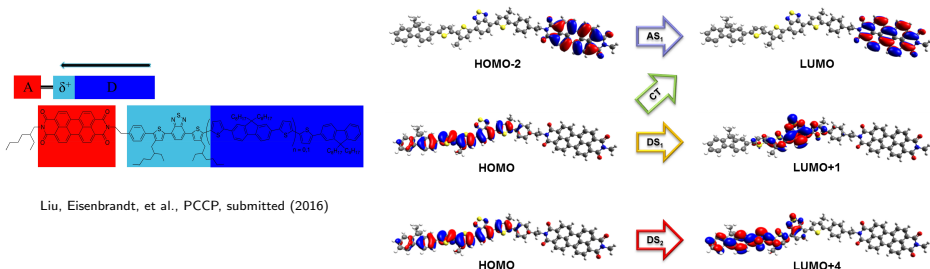
Roland, Ramirez, Léonard et al., PCCP, 14, 273 (2012)



Wenzel, Dreuw, Burghardt, PCCP, 15, 11704 (2013)

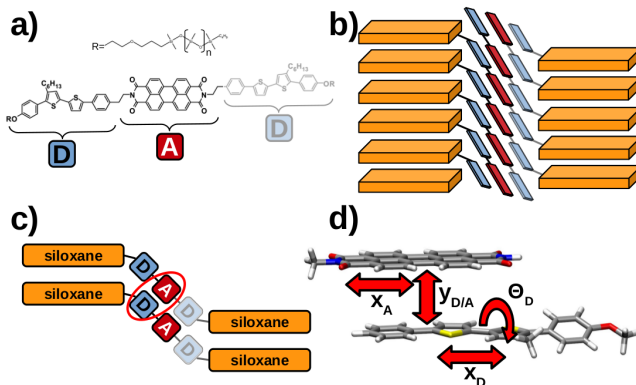
- competing ultrafast energy transfer (EET) and charge transfer (CT) processes
- in chloroform: **EET in 130 fs**, followed by **CT in 2.7 ps**
- in liquid crystalline phase: **CT in 60 fs!**
- relatively fast recombination (50 ps) – material doesn't really work well ...

Second Generation Material: Chemical Design



- concept: increase CT lifetime while preserving CT formation efficiency
- add benzothiadiazol spacer (δ^+) as well as amino (δ^-) moiety
- EET switched off, CT in 90 ps
- slow recombination – better performance than first-generation material
- morphology: lamellar mesophase rather than LC phase

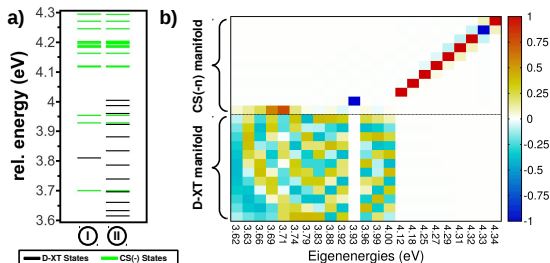
What is Happening in the First-Generation Material?



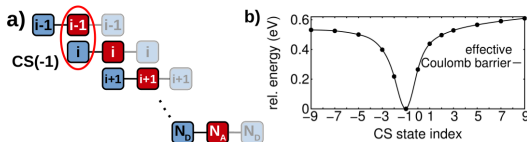
Polkehn et al., J. Phys. Chem. Lett.,
 DOI:10.1021/acs.jpclett.6b00277

- first-generation material: liquid crystalline smectic mesophase
- idea: D/A stacks serve as “quantum wells” for carrier transport
- much faster charge transfer in film than solution (~ 50 fs vs. ~ 3 ps)
- calculations suggest unexpected inter-chain D-A interactions

Liquid Crystalline Phase – Energetics



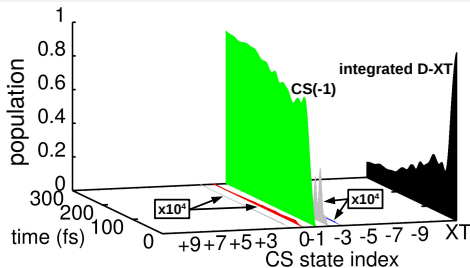
- energetics at Franck-Condon geometry
- state mixing: excitonic manifold and CS(-1) state
- but higher charge separated states barely accessible



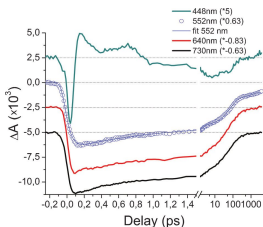
- on-site energies computed from ADC(2) and TDDFT
- internal field: $20 \text{ V}/\mu\text{m}$
- CS(-1) state strongly stabilized

Polkehn, Tamura, Eisenbrandt, Haacke, Méry, Burghardt, J. Phys. Chem. Lett., DOI:10.1021/acs.jpclett.6b00277

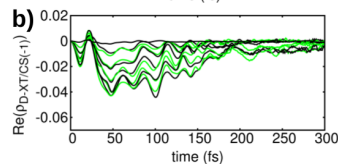
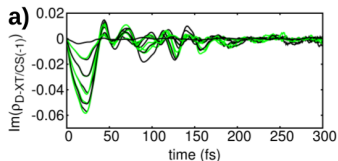
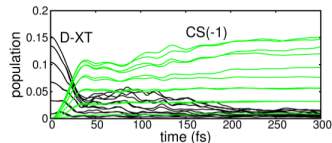
Liquid Crystalline Phase – Dynamics



Polkehn et al., JPCL (2016)



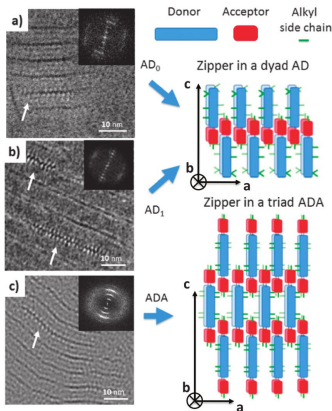
Roland et al., PCCP (2012)



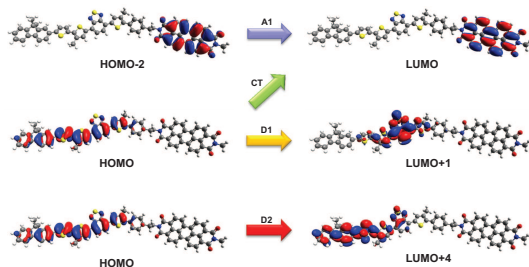
- transition to CS(-1) states (~ 50 fs) explains transient absorption experiments (Haacke)

- ML-MCTDH simulations for 156 states/48 modes

Second Generation Material: Zipper-like Molecular Packing



Biniek et al., J. Mater. Chem. C 3, 3342 (2015)

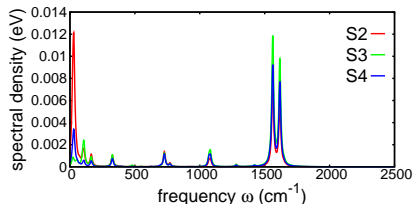
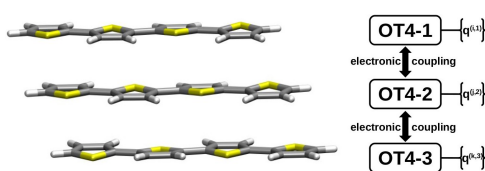


Liu, Eisenbrandt et al., PCCP, submitted

- tunable donor species: alternating thiophene/fluorene/benzothiadiazole units; electrodeficient bridge to the perylene acceptor
- organization in lamellae (both DA and ADA – but not DAD)
- comparatively slow CT formation (tens of ps); less recombination

Charge Transfer Excitons in Neat Regioregular Polythiophene

Reid et al., Chem. Mater. 26, 561 (2014), recent study by Lienau group [De Sio et al., Science, submitted]

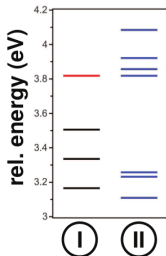
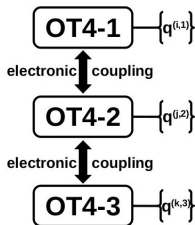


Polkehn, Tamura, Burghardt, in preparation

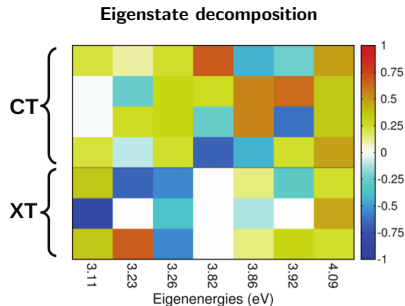
- inter-chain charge separation favored in PT (as compared with, e.g., PPV)
- electronic structure (ADC(2), TDDFT): low-energy inter-chain CT states
- electron-phonon coupling: spectral densities (*via* Franck-Condon gradient)
- representative quantum dynamics calculations for (OT)_n, $n = 3, 5$
- multiconfigurational quantum dynamics¹ for 9 electronic states, 270 modes

¹Multi-Layer Multi-Configuration Time-Dependent Hartree (ML-MCTDH)

Charge Transfer Excitons in Regioregular Oligothiophene



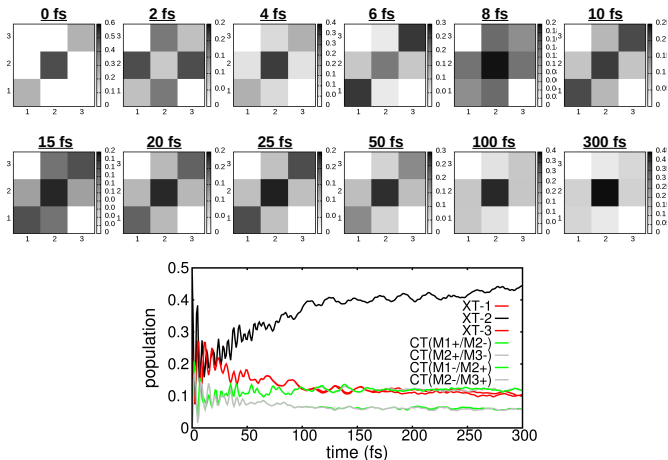
I: diabatic, II: adiabatic



Polkehn, Tamura, Burghardt, in preparation

- strong state mixing evidenced by electronic structure calculations
- excitonic ($J = 0.12$ eV) and exciton-CT ($K = 0.23$ eV) interactions
- bright state S_2 (H-aggregate) strongly mixed with CT states
- significant electron-phonon coupling

Dynamics of Charge Transfer Exciton Formation

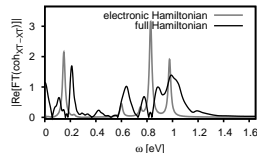
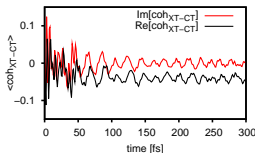
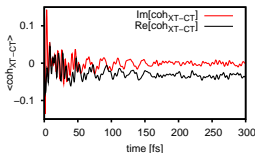


- coherent vibronic dynamics of electron-hole states
- quasi-stationary state: $\sim 40\%$ participation of charge transfer states
- time scale in good agreement with experiment [De Sio et al., submitted]

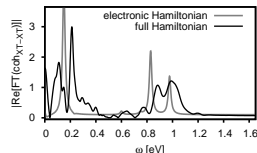
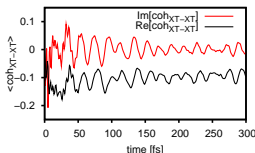
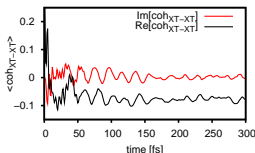
Marked Signature of Vibronic Coherence

Polkehn, Tamura, Burghardt, to be submitted

XT-CT
coherence



XT-XT
coherence



delocalized

vs.

localized initial condition

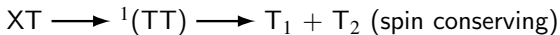
- relatively long-lasting coherent vibronic evolution
- sensitive dependence on initial condition (localized vs. delocalized exciton)
- Fourier Transform resembles electronic spectrum but exhibits Fano lineshapes
- dominant frequency around 0.2 eV is of vibronic, not pure vibrational origin

Topics

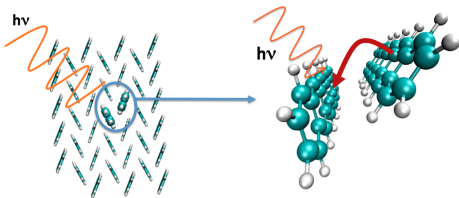
- 1 Photoinduced Energy & Charge Transfer in Functional Organic Materials
Goal: First-Principles Approach to Organic Photovoltaics
Electron-Hole Lattice Models & Electron-Phonon Coupling
Quantum Dynamics in Many Dimensions
- 2 Case Studies I: Charge Separation in Organic Photovoltaics
Oligothiophene-Fullerene (P3HT:PCBM Type) Junctions
Highly Ordered Oligothiophene-Perylene Assemblies
Charge Transfer Excitons in Neat Polythiophene
- 3 Case Studies II: Singlet Exciton Fission, Exciton Migration
Singlet Exciton Fission: Pentacene and Rubrene
Exciton Transport across Geometric Defects: Torsion-Induced EET
Summary & Outlook

Singlet Fission: Route To Carrier Multiplication

(collaboration with H. Tamura (Sendai), D. Beljonne (Mons))



possibly overcome to Shockley-Queisser limit

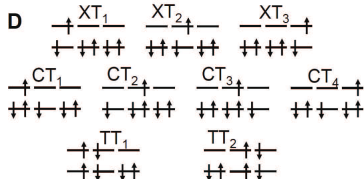
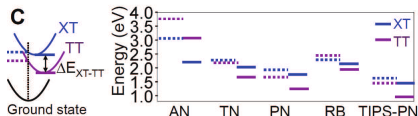


<http://sites.lsa.umich.edu/zimmerman-lab/wp-content/uploads/sites/52/2014/03>

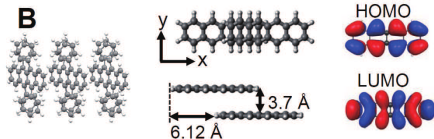
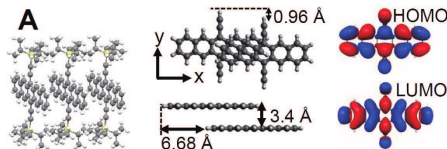
- driving force $\Delta E_{XT-TT} < 0$ doesn't explain the whole picture
- possible involvement of intermediate CT states (superexchange)
- vastly different time scales for different materials

- discovered in 1965: anthracene
- reviews by Smith & Michl, Annu. Rev. Phys. Chem. 2013, 64, 361, Chem. Rev. 110, 6891 (2010)

Molecular Packing: Energetics & Electronic Couplings



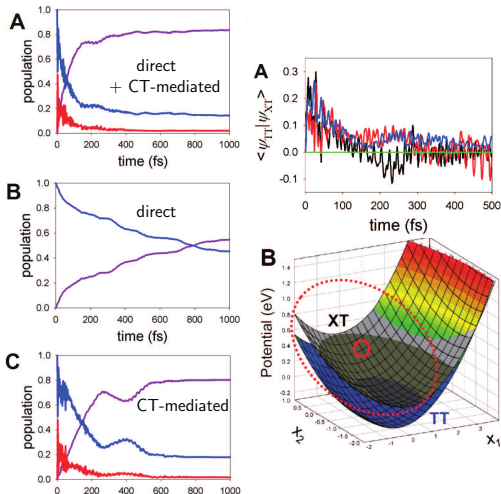
- energetics of acene series (C)
- trimer model: 9 states (D)



- TIPS-pentacene (A): slip-stacked
- rubrene (B): C_{2h} symmetric

Electronic coupling @ equil. non-zero for TIPS-pentacene but vanishing for rubrene!
(MRMP2 calculations for dimers, el. couplings via diabatisation protocol)

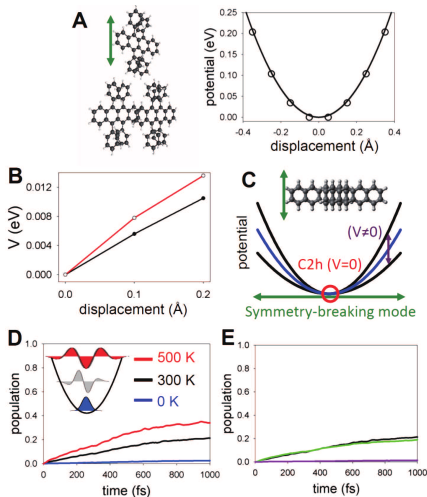
TIPS-Pentacene: Ultrafast Singlet Fission



- ultrafast, coherent SF
- slip-stacked geometry: avoided crossing
- interfering direct and CT-mediated pathways (electronic coupling via CT's dominates)
- vibrational coherence effectively transferred between XT and TT states (see $\langle \psi_{TT} | \psi_{XT} \rangle$)
- MRMP2 calculations + diabaticization

Musser et al., Nature Phys. 11, 352 (2015)

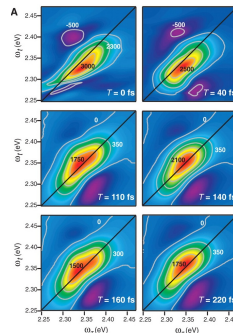
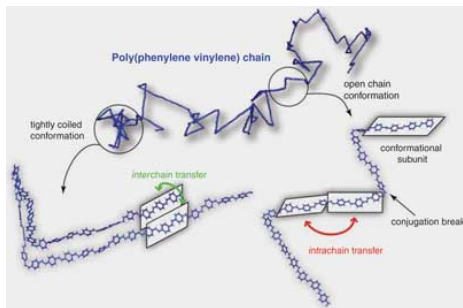
Rubrene: Thermally Activated Singlet Fission



- driving force slightly exergonic (like tetracene), but thermally activated SF (picosecond scale)
- C_{2h} crystal geometry: electronic coupling vanishes – conical intersection
- electronic couplings depend on symmetry-breaking coordinate: $V(X) = \lambda X$, $\lambda \sim 10^{-3}$ eV
- slow, incoherent dynamics
- key influence of molecular packing

Tamura, Huix-Rotllant, Burghardt, Olivier, Beljonne, Phys. Rev. Lett., 115, 107401 (2015)

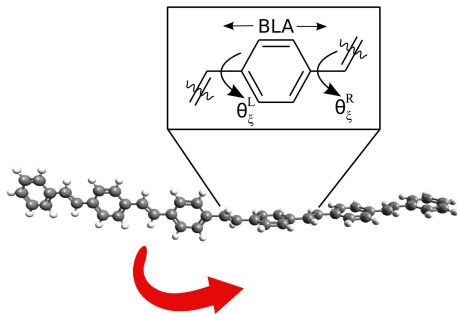
Exciton-Polarons in Organic Semiconducting Polymers



Collini, Schöles, Science 323, 369 (2009)

- ~0.1-1 ps: coherent intra-chain excitation energy transfer (EET) dynamics
- ~0.1-1 ps: self-trapped exciton-polaron states
- ~0.1-few ps: torsional geometry relaxation interfering with EET
- ~1-10 ps: inter-chain EET
- ~ps-ns: thermally assisted hopping

Test Case: Exciton Migration at a Torsional Defect



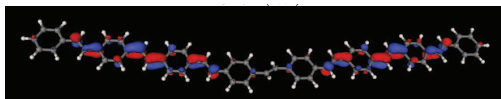
- full quantum dynamical study for minimal oligomer model
- MCTDH (up to 36 states, 22 vibrational modes)
- monomer-based diabatic Hamiltonian
- *ab initio* based parametrization

Binder, Wahl, Römer, Burghardt,
 Faraday Discuss 163, 205 (2013)
 Panda, Plasser, Aquino, Burghardt, Lischka
 J. Phys. Chem. A, 117, 2181 (2013)

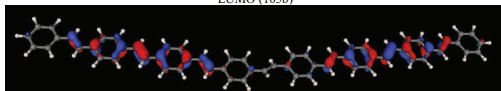
- Is a Frenkel exciton model ($|\Psi_{\text{exciton}}\rangle = \sum_n^{n_{\text{exc}}} c_n |\Phi_n\rangle$) sufficient?
- Is the transfer dynamics on ultrafast time scales **coherent** or of hopping type?
- What is the role of **electron-phonon** coupling?
- Is a trapped **exciton-polaron** generated and if so, on which time scale?

Electronic Structure of Oligomers (OPV's)

(Collaboration Lischka group (Texas Tech))

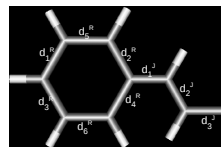
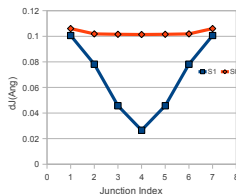
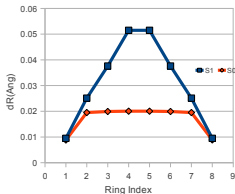


LUMO (105b)



HOMO (106a)

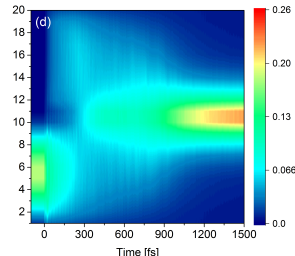
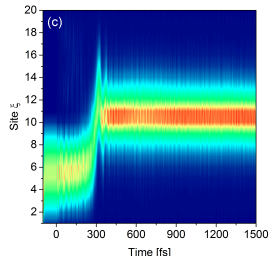
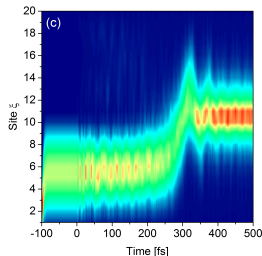
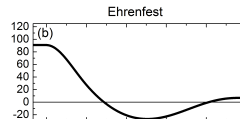
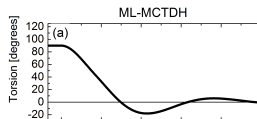
- high-level electronic structure methods (ADC, CC2, MRCI)
- exciton trapping, due to BLA modes, described correctly



Panda, Plasser, Aquino, Burghardt, Lischka, JPCA, 117, 2181 (2013), see also: Sterpone, Rossky, JPCB 112, 4983 (2008), Nayyar et al., JPCL 2, 566 (2011)

Coherent Exciton-Polaron “Hopping”

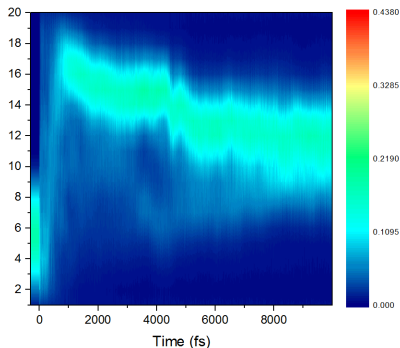
Wahl, Binder, Hegger, Burghardt, to be submitted



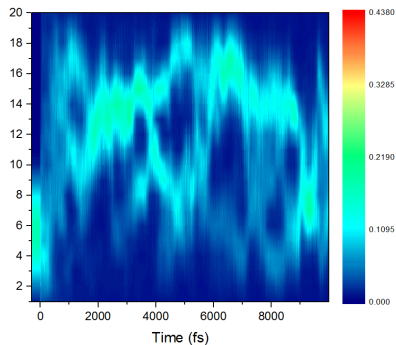
- transition between LEGSs = Local Exciton Ground States Tozer, Barford, JPCA (2012)
- ultrafast (~ 100 fs) transient between initial and final LEGS
- highly correlated dynamics not correctly reproduced by Ehrenfest approach

Exciton Migration – Ehrenfest/Langevin Dynamics

10 K



100 K



- mean-field Ehrenfest Dynamics (20 Frenkel states, 20 torsions/BLA's)
- trapped state at low temperatures
- at increasing temperatures, fluctuations start driving exciton migration

Wahl, Binder, Hegger, Burghardt, to be submitted

Summary

① Towards a Molecular-Level Control of Organic Photovoltaics

- combine model Hamiltonians & electronic structure information
- e - h lattice model: highlights “chemical control” + molecular packing
- possible future approach: coherent control by tailored laser fields

Summary

① Towards a Molecular-Level Control of Organic Photovoltaics

- combine model Hamiltonians & electronic structure information
- e - h lattice model: highlights “chemical control” + molecular packing
- possible future approach: coherent control by tailored laser fields

② Charge Separation at Donor-Acceptor Junctions

- ultrafast (~ 50 - 100 fs), coherent initial charge separation
- Coulomb barrier to free carrier formation of key importance
- quasi-stationary polaronic states on ~ 1 ps time scale

Summary

① Towards a Molecular-Level Control of Organic Photovoltaics

- combine model Hamiltonians & electronic structure information
- e - h lattice model: highlights “chemical control” + molecular packing
- possible future approach: coherent control by tailored laser fields

② Charge Separation at Donor-Acceptor Junctions

- ultrafast (~ 50 - 100 fs), coherent initial charge separation
- Coulomb barrier to free carrier formation of key importance
- quasi-stationary polaronic states on ~ 1 ps time scale

③ Singlet Fission, Exciton Migration

- singlet exciton fission depends crucially on molecular packing
- exciton migration *via* “coherent hopping” dynamics
- ultrafast formation of quasi-stationary exciton-polaron states

Summary

① Towards a Molecular-Level Control of Organic Photovoltaics

- combine model Hamiltonians & electronic structure information
- e - h lattice model: highlights “chemical control” + molecular packing
- possible future approach: coherent control by tailored laser fields

② Charge Separation at Donor-Acceptor Junctions

- ultrafast (~ 50 - 100 fs), coherent initial charge separation
- Coulomb barrier to free carrier formation of key importance
- quasi-stationary polaronic states on ~ 1 ps time scale

③ Singlet Fission, Exciton Migration

- singlet exciton fission depends crucially on molecular packing
- exciton migration *via* “coherent hopping” dynamics
- ultrafast formation of quasi-stationary exciton-polaron states

Acknowledgments & Collaborations

Group Frankfurt:

- M. Biswas
- P. Mondal
- D. Rastädter
- R. Binder
- J. Wahl
- P. Eisenbrandt
- M. Polkehn
- M. Huix-Rotllant

Former members:

- S. Römer
- M. Ruckebauer
- J. Ortiz-Sánchez

Collaborations:

- H. Tamura (Sendai, Japan)
- K. H. Hughes (Bangor, UK)
- R. Martinazzo (Milano, Italy)
- H. Lischka, A. Aquino (TTU, USA)
- F. Plasser (Heidelberg, Germany)
- J. Wenzel, A. Dreuw (Heidelberg, Germany)
- S. Haacke, S. Méry (Strasbourg, France)
- F. Sterpone (IBPC, Paris)
- E. R. Bittner (Houston University, USA)
- L. S. Cederbaum (Heidelberg, Germany)
- A. Panda (IIT Guwahati, India)
- D. Beljonne, Y. Olivier (Mons, Belgium)

Thanks to: DFG, CNRS, ANR (France) for financial support





Theoretical Chemistry
of Complex Systems

AK Burghardt



How Fast is Decoherence?

$$|\psi(t)\rangle = c_0(t)|0\rangle|\phi_0(t)\rangle + c_1(t)|1\rangle|\phi_1(t)\rangle$$

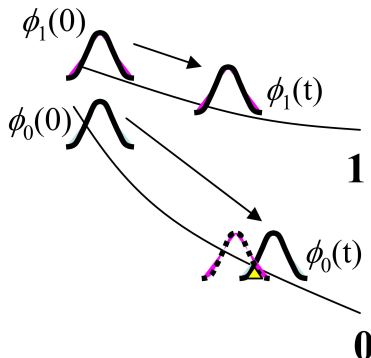
electronic coherence:

$$\begin{aligned}\rho_{01}(t) &= \text{Tr}[|0\rangle\langle 1|\hat{\rho}(t)] \\ &= \langle 1|\hat{\rho}(t)|0\rangle = c_1^*(t)c_0(t)\langle\phi_1(t)|\phi_0(t)\rangle\end{aligned}$$

- coherence \propto overlap of nuclear wavefunctions
- typical decoherence times: ~ 30 fs
 (estimate from $\tau_{\text{dec}} \sim \tau_g(6k_B T/\lambda)^{1/2}$
 or $\tau_{\text{dec}} \sim \gamma^{-1}(\lambda_T/\Delta x)^2$)

Prezdho, Rossky, PRL 81, 5294 (1998)

- loss of coherence *not* captured by classical trajectory picture



picture: P. Rossky et al.

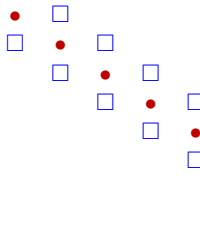
Spectral Densities as Continued Fractions

- map spectral densities onto the transformed representation
- “Mori-chain” continued fraction (CF):

$$J(\omega) = \frac{\pi}{2} \sum_n \frac{c_n^2}{\omega_n} \delta(\omega - \omega_n) \quad \longleftrightarrow \quad J(\omega) = \lim_{\varepsilon \rightarrow 0^+} \operatorname{Im} K(z) \Big|_{z=\omega-i\varepsilon}$$

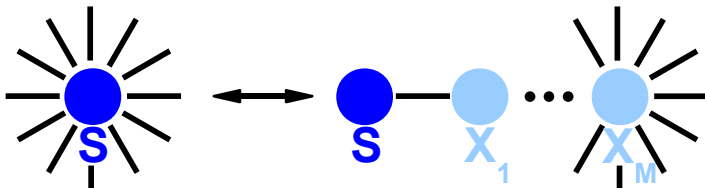
- CF poles yield multi-exponential form of correlation functions

Hughes, Christ, Burghardt, JCP 131, 024109 (2009), Garg, Onuchic, Ambegaokar, JCP 83, 4491 (1985), Leggett, Phys. Rev. B 30, 1208 (1984)



$$K(z) = - \frac{D^2}{\Omega_1^2 - z^2 - \frac{d_{1,2}^2}{\Omega_2^2 - z^2 - \dots - \frac{d_{M-2,M-1}^2}{\Omega_{M-1}^2 - z^2 - \dots}}}$$

Effective-Mode Decomposition of Phonon Space

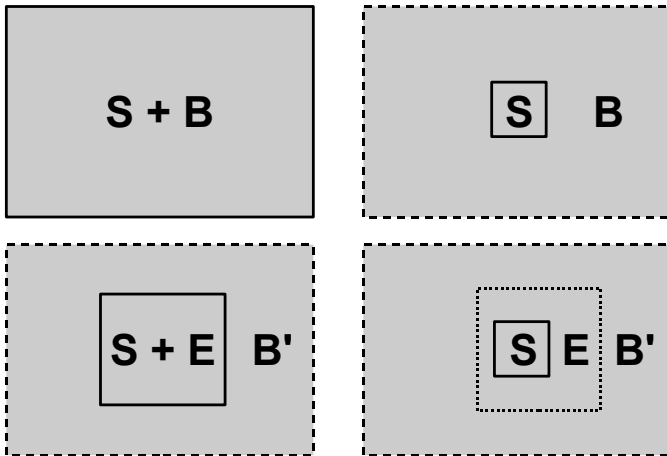


Martinazzo, Vacchini, Hughes, Burghardt, J. Chem. Phys. 134, 011101 (2011), Hughes, Christ, Burghardt, J. Chem. Phys. 131, 024109 (2009)
 Tamura, Bittner, Burghardt, J. Chem. Phys. 126, 021103 (2007), Gindensperger, Köppel, Cederbaum, J. Chem. Phys. 126, 034106 (2007)
 Cederbaum, Gindensperger, Burghardt, Phys. Rev. Lett., 94, 113003 (2005), Garg, Onucic, Ambegaokar, J. Chem. Phys. 83, 4491 (1985)

$$\hat{H}_{SB} + \hat{H}_B = \hat{s} \sum_i c_n \hat{x}_n + \hat{H}_B \longrightarrow D \hat{s} \hat{X}_1 + d_{12} \hat{X}_1 \hat{X}_2 + \dots + \hat{X}_M \text{--residual bath}$$

- orthogonal coordinate transformation $\hat{X} = \mathbf{T}\hat{x}$
- short-time dynamics captured by first few effective modes
- truncate hierarchical chain to define approximate reduced-dimensional model
- similarity to t-DMRG technique

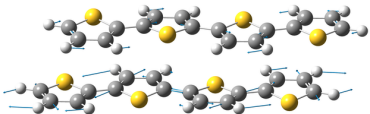
System-Bath Partitionings



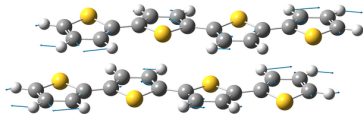
S = system, B = bath, E = effective-mode part of the bath

Oligothiophene Modes

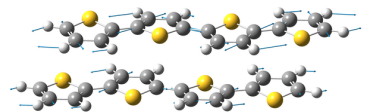
1561 cm^{-1}



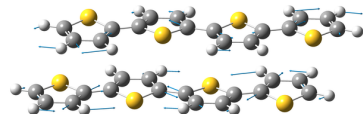
1616 cm^{-1}



1562 cm^{-1}



1617 cm^{-1}



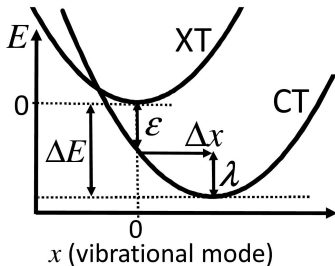
Linear Vibronic Coupling (LVC) model

$$\hat{H} = \hat{H}_0 + \hat{H}_R + \hat{H}_B$$

\hat{H}_0 : electronic part

\hat{H}_R : inter-fragment coordinate part

\hat{H}_B : phonon bath part



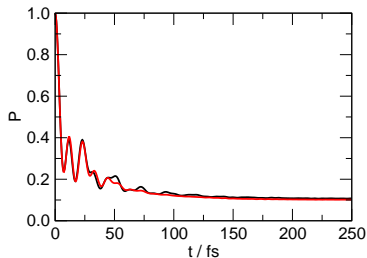
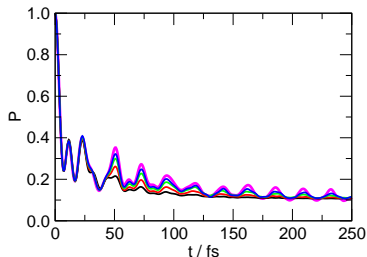
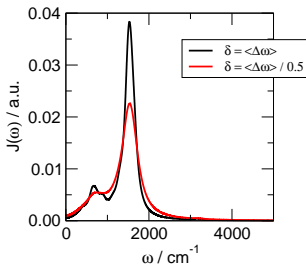
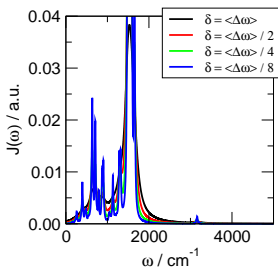
$$\hat{H}_0 = \Delta_{\text{XT-CT}} |\text{CT}\rangle \langle \text{CT}| + \gamma (|\text{XT}\rangle \langle \text{CT}| + |\text{CT}\rangle \langle \text{XT}|)$$

$$\begin{aligned} \hat{H}_R = & \frac{\omega_R}{2} (\hat{R}^2 + \hat{P}^2) + \kappa_R \hat{R} |\text{CT}\rangle \langle \text{CT}| \\ & + \gamma_R \hat{R} (|\text{XT}\rangle \langle \text{CT}| + |\text{CT}\rangle \langle \text{XT}|) \end{aligned}$$

$$\hat{H}_B = \sum_{i=1}^N \frac{\omega_i}{2} (\hat{x}_i^2 + \hat{p}_i^2) + \sum_{i=1}^N \kappa_i x_i |\text{CT}\rangle \langle \text{CT}| + \sum_{i=1}^N \frac{\kappa_i^2}{2\omega_i}$$

Oligothiophene-Fullerene Junction: Quantum Dynamics

spectral density



XT population

- MCTDH calculations (2 states, 61 modes); coherent features over initial 50 fs

Coherence & Decoherence

$$|\psi(t)\rangle = c_0(t)|0\rangle|\phi_0(t)\rangle + c_1(t)|1\rangle|\phi_1(t)\rangle$$

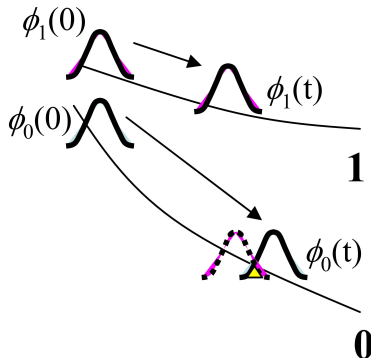
electronic coherence:

$$\begin{aligned}\rho_{01}(t) &= \text{Tr}[|0\rangle\langle 1|\hat{\rho}(t)] \\ &= \langle 1|\hat{\rho}(t)|0\rangle = c_1^*(t)c_0(t)\langle\phi_1(t)|\phi_0(t)\rangle\end{aligned}$$

- coherence \propto overlap of nuclear wavefunctions
- typical decoherence times: ~ 30 fs
(estimate from $\tau_{\text{dec}} \sim \tau_g(6k_B T/\lambda)^{1/2}$
or $\tau_{\text{dec}} \sim \gamma^{-1}(\lambda_T/\Delta x)^2$)

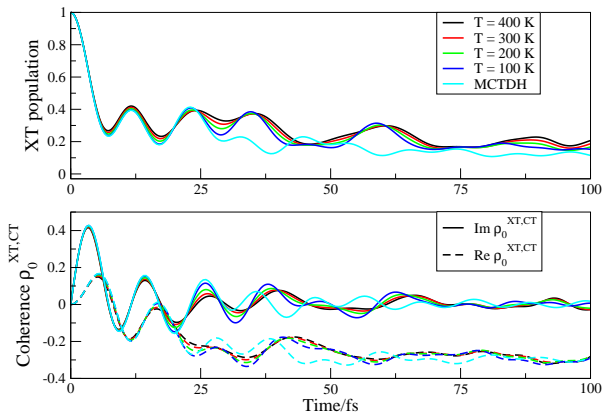
Prezdho, Rossky, PRL 81, 5294 (1998)

- loss of coherence *not* captured by classical trajectory picture



picture: P. Rossky et al.

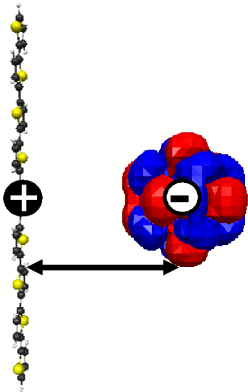
Temperature Dependence Not a Key Factor



- Hierarchical Equations of Motion (HEOM) approach Tanimura, J. Phys. Soc. Jpn. **75**, 082001 (2006)
- reduced dynamics + effective mode decomposition Burghardt et al., JCP **137**, 144107 (2012)
- experiments show negligible temperature dependence Pensack, Asbury, JACS **131**, 15986 (2009)

Hughes, Cahier, Martinazzo, Burghardt, Chem. Phys., Femto 2013 issue, <http://dx.doi.org/10.1016/j.chemphys.2014.06.015>

Free Carrier Generation, Cont'd



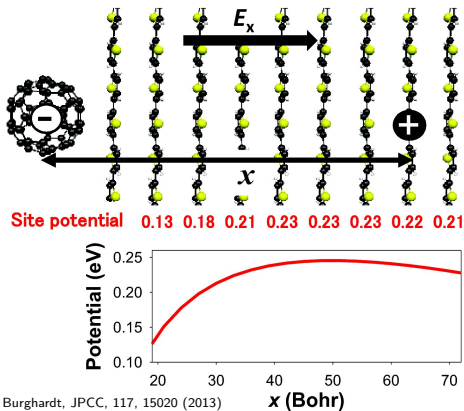
- analytical e - h potential
(interaction point charge/charged rod):

$$\phi(x) = -(1/(\epsilon_r a))[\ln(a + \sqrt{a^2 + x^2}) - \ln x] - E_x x$$

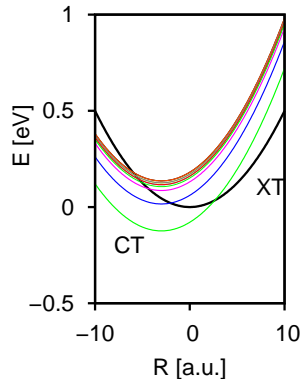
Tamura, Burghardt, J. Phys. Chem. C, 117, 15020 (2013)
- Coulomb potential becomes shallower as the conjugation length (a) increases
- connection to analysis by Deibel/Dyakonov:¹ conjugated chain segments favor charge separation
- barrier height ~ 0.5 eV ($E_x = 10$ V/ μm),
 ~ 0.3 eV ($E_x = 50$ V/ μm)
- additional effect: barrier height also decreases as a function of fullerene aggregation

¹Deibel et al., PRL 103, 036402 (2009) "Origin of the Efficient Polaron-Pair Dissociation in Polymer-Fullerene Blends"

Free Carrier Generation, cont'd

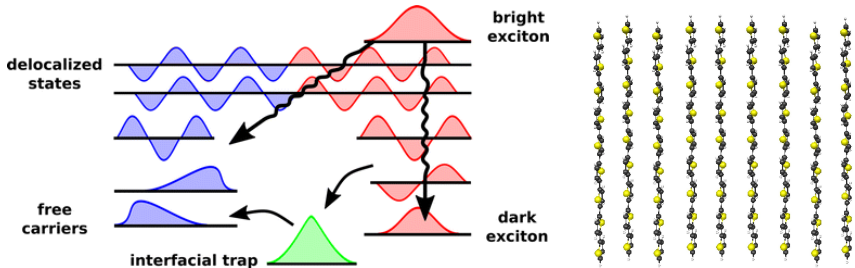


Tamura, Burghardt, JPCC, 117, 15020 (2013)



- lamellar stacking (regio-regular structure)
- Coulomb barrier determines on-site energy of charge separated (CS) states
- excess energy favors $e-h$ separation; depends on initial state

What is the Role of Exciton Delocalization?



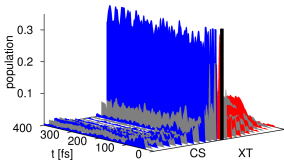
- manifolds of excitonic (H-aggregate type) and charge transfer states
- interfacial “trap” possibly bypassed?
- recent experiments: ultrafast generation of free carriers
- also: ultrafast free carrier generation by direct excitation of trapped state

Gélinas et al., Science 343, 512 (2014), Vandewal et al., Nature Mater. 13, 63 (2014)
Huix-Rotllant, Tamura, Burghardt, J. Phys. Chem. Lett., 6, 1702 (2015)

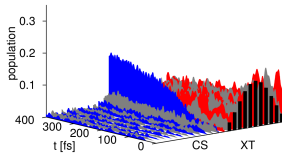
Bright States Partially Circumvent Interfacial Traps

$$\hat{H} = \hat{H}_{\text{XT}_1\text{-CT}}(\mathbf{x}) + \sum_n \hat{H}_{\text{CS}}^{(n)}(\mathbf{x}) |\text{CS}_n\rangle \langle \text{CS}_n| + t(\mathbf{x}) (|\text{CS}_1\rangle \langle \text{CT}| + \sum_{nn'} |\text{CS}_n\rangle \langle \text{CS}_{n'}| + h.c.) \\ + \sum_n \hat{H}_{\text{XT}}^{(n)}(\mathbf{x}) |\text{XT}_n\rangle \langle \text{XT}_n| + j(\mathbf{x}) \sum_{nn'} (|\text{XT}_n\rangle \langle \text{XT}_{n'}| + h.c.)$$

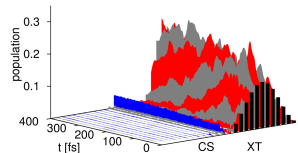
CT/CS states: blue/grey, XT: red/grey



(1) localized initial exciton



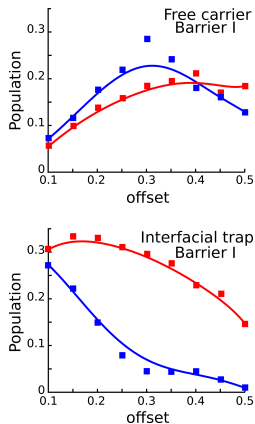
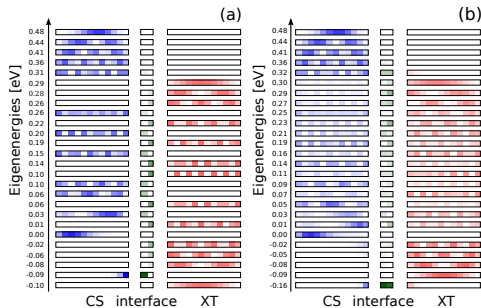
(2) bright initial exciton



(3) dark initial exciton

- CT/CS generation depends on exciton (de)localization
- H aggregate (here, oligothiophene): upper exciton state is bright
- localized initial condition permits efficient transfer
- bright XT can decay to dark XT, which is in turn ineffective at charge transfer

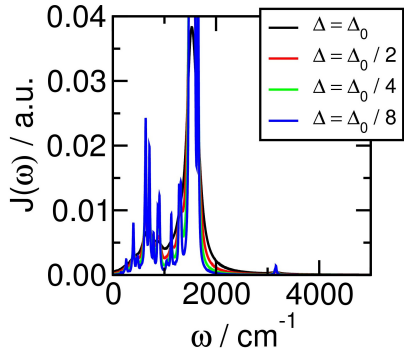
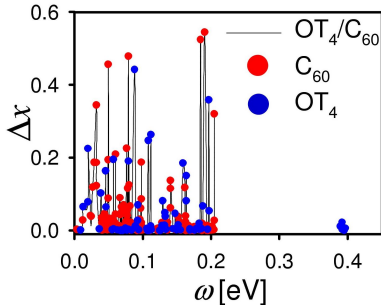
Electronic Eigenstate Picture



- interplay of delocalization, internal conversion, and charge transfer
- de/localized initial condition (blue/red) reduces/enhances interfacial trapping

Huix-Rotllant, Tamura, Burghardt, J. Phys. Chem. Lett., 6, 1702 (2015)

Oligothiophene-Fullerene Junction: Spectral Density



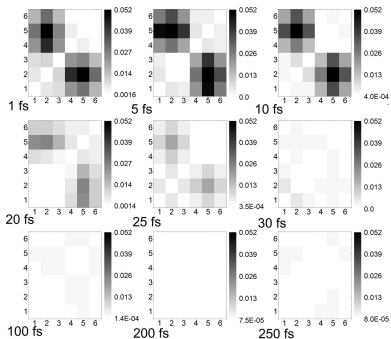
$$J(\omega) = \frac{\pi}{2} \sum_n^N \frac{c_n^2}{\omega_n} \delta(\omega - \omega_n)$$

$$J(\omega) \simeq \frac{\pi}{2} \sum_n^N \frac{c_n^2}{\pi} \frac{\Delta}{(\omega - \omega_n)^2 + \Delta^2}$$

Tamura, Martinazzo, Ruckebauer, Burghardt, J. Chem. Phys., 137, 22A540 (2012)

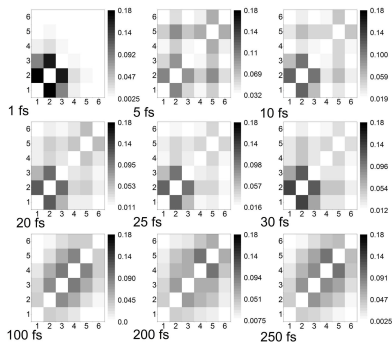
Coherence Evolution

$$\text{Im}\rho_{vv,\mu\mu}(t) = \text{Im}\text{Tr}\{|vv\rangle\langle\mu\mu|\hat{\rho}(t)\}$$



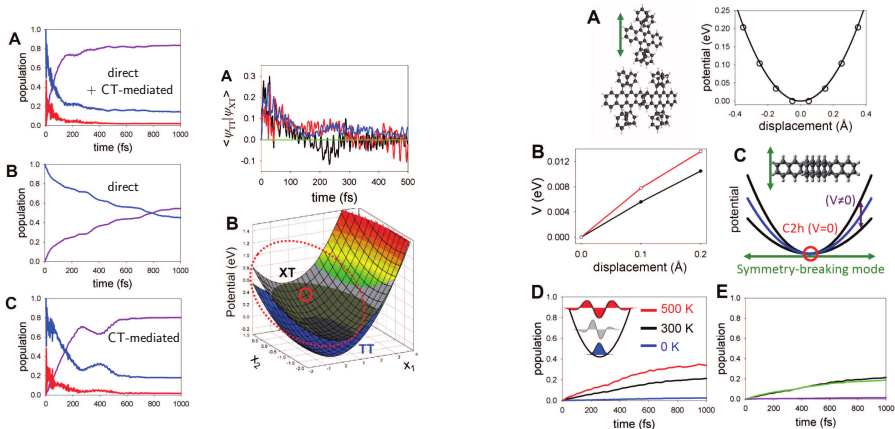
- **Imaginary** part \leftrightarrow population flux
- ultrafast decay time (~ 50 fs)

$$\text{Re}\rho_{vv,\mu\mu}(t) = \text{Re}\text{Tr}\{|vv\rangle\langle\mu\mu|\hat{\rho}(t)\}$$



- **Real** part \leftrightarrow stationary superposition
- reaches stationary LEGS coherence

Ultrafast vs. Thermally Activated Singlet Fission



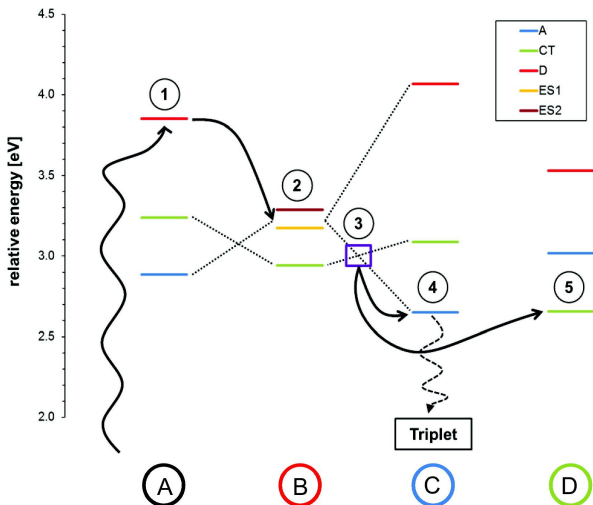
Tamura, Huix-Rotllant, Burghardt, Olivier, Beljonne, Phys. Rev. Lett., in press (2015), arXiv:1504.05088v1

- **TIPS-pentacene**: ultrafast, coherent SF
- slip-stacked geometry: avoided crossing
- both direct and CT-mediated pathways

- **rubrene**: thermally activated SF
- C_{2h} geometry: conical intersection
- role of symmetry-breaking modes

Dyad Electronic Structure

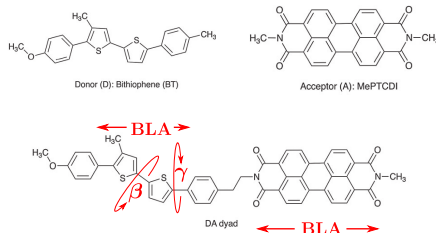
- LC-TDDFT calculations
- three relevant states:
 $D \equiv (D^*A)$
 $A \equiv (DA^*)$
 $CT \equiv (D^+A^-)$
- geometries:
 (A) = FC geometry
 (B) = A/D crossing:
excitonic $ES1/2$ states
 (C) = A minimum
 (D) = CT minimum
- CT state has 68 D (!)
dipole moment



J. Wenzel, A. Dreuw, I Burghardt, PCCP 15, 11704 (2013)

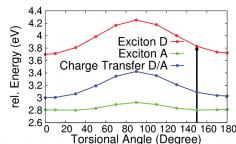
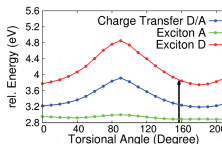
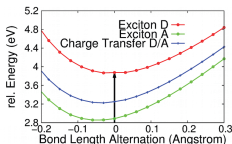
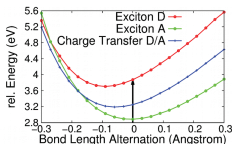
Active Coordinates

- select Franck-Condon active modes: bond length alternation (BLA) + torsional modes
- calculate anharmonic PES profiles for these modes



BLA donor

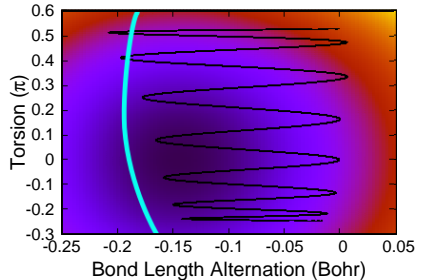
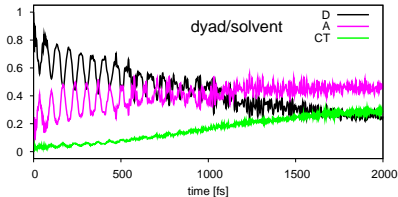
BLA acceptor

 β torsion donor γ torsion donor

$$V_i^{\text{BLA}}(x) = D_i(1 - \exp(-\kappa_i(r - r_0)))^2$$

$$V_i^{\text{torsion}}(\theta) = a_i + b_i \cos \theta + c_i \cos 2\theta + d_i \cos 4\theta$$

Dynamics in Solution

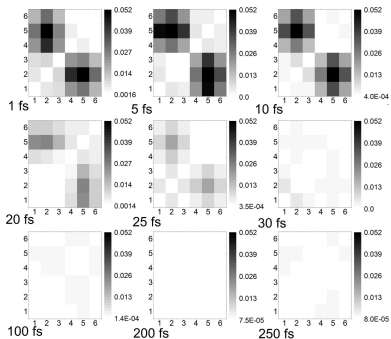


cyan: avoided crossing seam

- coherent interplay of high-frequency (BLA), low-frequency (torsion) modes, and solvent coordinate
- low-frequency modes tune high-frequency modes into vibronic resonance
- similar to “hybrid model” (Barbara and collaborators, JCP 96, 7859 (1992))
- diabatic D-CT and A-CT coupling small ($\sim 10^{-3}$ eV)

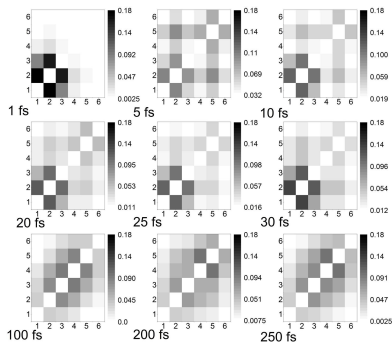
Coherence Evolution: Site Basis

$$\text{Im}\rho_{vv,\mu\mu}(t) = \text{Im Tr}\{|vv\rangle\langle\mu\mu|\hat{\rho}(t)\}$$



- **Imaginary** part \leftrightarrow population flux
- ultrafast decay time (~ 50 fs)

$$\text{Re}\rho_{vv,\mu\mu}(t) = \text{Re Tr}\{|vv\rangle\langle\mu\mu|\hat{\rho}(t)\}$$

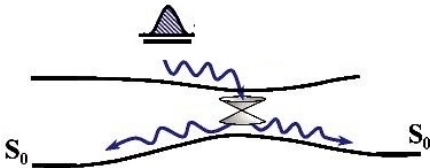


- **Real** part \leftrightarrow stationary superposition
- reaches stationary LEGS coherence

Conical Intersection: $3 \times n$ Effective Modes

Precursors in solid state physics:
 “cluster modes”
 “interaction modes”

(O'Brien 1971, Toyozawa, Inoue 1966)



electronic subsystem: $|i\rangle\langle j|$, $i, j = 1, 2$



primary effective modes $\{\hat{X}_1, \hat{X}_2, \hat{X}_3\}$



residual modes $\{\hat{X}_4, \dots, \hat{X}_N\}$

- several subsystem operators
- effective modes describe short-time dynamics exactly
- for n electronic states:
 $n(n+1)/2$ primary effective modes

Cederbaum, Gindensperger, Burghardt, Phys. Rev. Lett., **94**, 113003 (2005)

Burghardt, Gindensperger, Cederbaum, Mol. Phys. **104**, 1081 (2006)

Gindensperger, Burghardt, Cederbaum, J. Chem. Phys. **124**, 144104, 144105 (2006)

Electronic (De-)Coherence

$$|\psi(t)\rangle = c_0(t)|0\rangle|\phi_0(t)\rangle + c_1(t)|1\rangle|\phi_1(t)\rangle$$

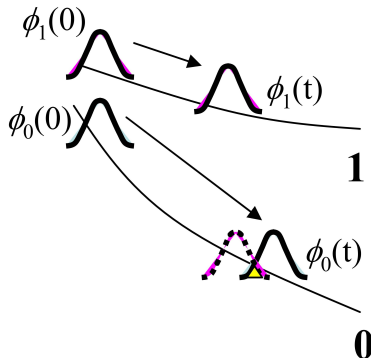
electronic coherence:

$$\begin{aligned}\rho_{01}(t) &= \text{Tr}[|0\rangle\langle 1|\hat{\rho}(t)] \\ &= \langle 1|\hat{\rho}(t)|0\rangle = c_1^*(t)c_0(t)\langle\phi_1(t)|\phi_0(t)\rangle\end{aligned}$$

- coherence \propto overlap of nuclear wavefunctions
- typical decoherence times: ~ 30 fs
(estimate from $\tau_{\text{dec}} \sim \tau_g(6k_B T/\lambda)^{1/2}$
or $\tau_{\text{dec}} \sim \gamma^{-1}(\lambda_T/\Delta x)^2$)

Prezdho, Rossky, PRL 81, 5294 (1998)

- loss of coherence *not* captured by classical trajectory picture



picture: P. Rossky et al.

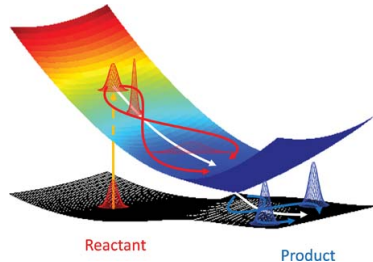
Quantum Dynamics in Many Dimensions – Key Issues

$$i\frac{\partial\Psi}{\partial t} = \hat{H}\Psi$$

$$i\frac{\partial\hat{\rho}}{\partial t} = [\hat{H}, \hat{\rho}] + \hat{L}_{\text{diss}}\hat{\rho}$$

- exponential scaling problem: $\sim fN^{f+1}$;
hence, standard basis set methods do not go beyond 5-6 degrees of freedom (DOF)^(*)
- construction of high-dimensional potential energy surfaces (PES) necessary
- wavepacket propagation not immediately compatible with on-the-fly (“direct dynamics”) approaches
- open systems: ultrafast processes generally fall into a non-Markovian regime

^(*)NB.: f = number of DOF's; N = grid dimension



www.cecarn.org/workshop-4-406.html?presentation-id=5680

Multiconfigurational Methods: MCTDH

$$\Psi(r, t) = \sum_J A_J(t) \Phi_J(r, t) \equiv \sum_{j_1=1}^{n_1} \dots \sum_{j_N=1}^{n_N} A_{j_1 \dots j_N}(t) \phi_{j_1}^{(1)}(r_1, t) \dots \phi_{j_N}^{(N)}(r_N, t)$$

- Multi-Configuration Time-Dependent Hartree: tensor approximation scheme
Meyer, Manthe, Cederbaum, Chem. Phys. Lett. **165**, 73 (1990), Beck et al., Phys. Rep. **324**, 1 (2000)
- EoM's from the Dirac-Frenkel variational principle: $\langle \delta \Psi | \hat{H} - i \frac{\partial}{\partial t} | \Psi \rangle = 0$
- MCTDH takes one to **50-100 modes**; exponential scaling alleviated
- restriction on the form of the potential: sums over products
- related multi-layer variant (**ML-MCTDH**) goes up to **1000 modes**
Wang, Thoss, J. Chem. Phys. **119**, 1289 (2003)
- related **MCTDH-F** (fermion) and **MCTDH-B** (boson) methods
Kato, Kono, Chem. Phys. Lett. **392**, 533 (2004), Nest, Klamroth, Saalfrank, J. Chem. Phys. **122**, 124102 (2005)
Alon, Streltsov, Cederbaum, Phys. Lett. A **362**, 453 (2007)
- **density matrix** variant
Raab, Burghardt, Meyer, J. Chem. Phys. **111**, 8759 (1999)
- **hybrid** approaches: e.g., Gaussian-based variant (**G-MCTDH**, **vMCG**)
Burghardt, Meyer, Cederbaum, J. Chem. Phys. **111**, 2927 (1999), Worth, Burghardt, Chem. Phys. Lett. **368**, 502 (2003)

Variationally Optimized Dynamics

$$\Psi(r_1, \dots, r_P, t) = \sum_{j_1} \dots \sum_{j_P} A_{j_1 \dots j_P}(t) \prod_{\kappa=1}^M \phi_{j_\kappa}^{(\kappa)}(r_\kappa, t) \prod_{\kappa=M+1}^P g_{j_\kappa}^{(\kappa)}(r_\kappa, t)$$

$$g_j^{(\kappa)}(r_\kappa, t) = \exp \left[r_\kappa \cdot a_j^{(\kappa)}(t) r_\kappa + \xi_j^{(\kappa)}(t) \cdot r_\kappa + \eta_j^{(\kappa)}(t) \right]$$

multidimensional Gaussian functions:

- “thawed” (TG) vs. “frozen” (FG)
- quasi-classical motion for $\xi_j = -2a_j q_j + ip_j$
- analytical integrals

Dirac-Frenkel **variational principle**:

$$\langle \delta \Psi | H - i \frac{\partial}{\partial t} | \Psi \rangle = 0 \longrightarrow \text{dynamical equations for } \Lambda_j^{(\kappa)} = (a_j^{(\kappa)}, \xi_j^{(\kappa)}, \eta_j^{(\kappa)})$$

- up to 50-100 modes – exponential scaling problem ($\sim fN^{f+1}$) is alleviated

Symplectic Structure of “VP Mechanics”

- variational formulation via action integral: $\delta \mathcal{S} = \delta \int dt \mathcal{L} = 0$

classical mechanics

$$\mathcal{L} = \sum_k p_k \dot{q}_k - H(q_k, p_k)$$

$$\dot{q}_k = \frac{\partial H}{\partial p_k}$$

$$\dot{p}_k = -\frac{\partial H}{\partial q_k}$$

VP mechanics

$$\mathcal{L} = \sum_{\alpha=1} S^{(0\alpha)} \dot{\lambda}_{\alpha} - \langle \Psi | H | \Psi \rangle$$

$$\text{identify: } \tilde{p}_{\alpha} = S^{(0\alpha)} = i \langle \Psi | \frac{\partial \Psi}{\partial \lambda_{\alpha}} \rangle$$

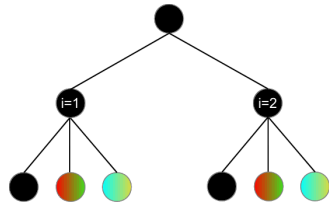
$$\begin{aligned} \dot{\lambda}_{\alpha} &= \frac{\partial \langle H \rangle}{\partial \tilde{p}_{\alpha}} \\ &= \sum_{\beta} \frac{\partial \langle H \rangle}{\partial \lambda_{\beta}} \frac{\partial \lambda_{\beta}}{\partial \tilde{p}_{\alpha}} \\ &= \sum_{\beta} \frac{\partial \langle H \rangle}{\partial \lambda_{\beta}} \left(C^{-1} \right)_{\alpha\beta} \end{aligned}$$

Two-Layer (2L)-G-MCTDH Scheme

$$\Psi(r, t) = \sum_J A_J(t) \Phi_J(r, t) = \sum_J A_J(t) \prod_{\kappa=1}^M \varphi_{j_\kappa}^{(\kappa)}(r_\kappa, t)$$

where the single-particle functions (SPFs) $\varphi_{j_\kappa}^{(\kappa)}$ are now built as superpositions of Frozen Gaussian (FG) configurations,

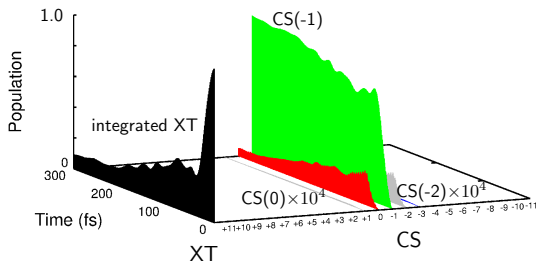
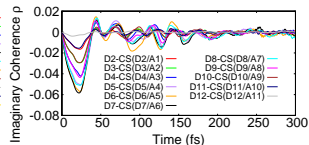
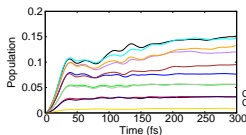
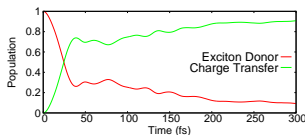
$$\begin{aligned} \varphi_{j_\kappa}^{(\kappa)}(r_\kappa, t) &= \sum_L B_{j,L}^{(\kappa)}(t) G_L^{(\kappa)}(r_\kappa, t) \\ &= \sum_L B_{j,L}^{(\kappa)}(t) \prod_{\mu} g_{l_\mu}^{(\kappa, \mu)}(r_{\kappa_\mu}, t) \end{aligned}$$



- “hierarchical Tucker format”
- intra-SPF correlations are carried by B coefficients
- GWP parameter dynamics in small (κ, μ) subspaces
- first-layer SPFs can be chosen to be orthogonal: $\langle \varphi_j^{(\kappa)}(t) | \varphi_{j'}^{(\kappa)}(t) \rangle = \delta_{jj'}$

Römer, Ruckebauer, Burghardt, J. Chem. Phys. 138, 064106 (2013)

Liquid Crystalline Phase – Dynamics



- ML-MCTDH calculations (120 electronic states, 39 modes) incl. inter-chain modes

- ultrafast population of charge separated states
- initial excitation to the lower edge of the J-type donor excitonic manifold
- unfavorable transfer integrals ($\sim 10^{-4}$) prevent formation of CS(n) states with $|n| > 1$
- experimental observation: recombination on ~ 50 ps time scale

Polkehn et al., to be submitted

Approximate Wavefunctions from the Dirac-Frenkel Variational Principle

Dirac-Frenkel (DF) **variational principle**:

$$\langle \delta\Psi | \hat{H} - i \frac{\partial}{\partial t} | \Psi \rangle = 0 \longrightarrow \text{dynamical equation for } \dot{\Psi}$$

where $\delta\Psi \in \mathcal{T}_{\Psi}\mathcal{M}$ (tangent space wrt the approximate manifold \mathcal{M} on which the wavefunction is defined)

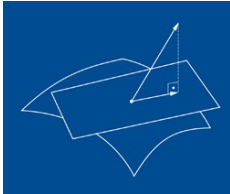
Dirac 1930, Frenkel 1934, McLachlan 1964

- the time derivative is then given by

$$\dot{\Psi} = \mathcal{P}(\Psi) \frac{1}{i} \hat{H} \Psi$$

where $\mathcal{P}(\Psi)$ projects onto the tangent space

- the residual is minimized: $\|\dot{\Psi} - \frac{1}{i} \hat{H} \Psi\| = \min$
- norm conservation, energy conservation
- symplectic flow



C. Lubich, From Quantum to Classical Molecular Dynamics: Reduced Models and Numerical Analysis, Zürich (2008)

Multi-Configuration Time-Dependent Hartree (MCTDH)

- standard basis set methods do not go beyond 5-6 dimensions ($\sim fN^{f+1}$)
- approximate Ψ by an *ansatz*: linear combination of Hartree products

$$\begin{aligned}\Psi(r, t) &= \sum_J A_J(t) \Phi_J(r, t) \\ &= \sum_{j_1=1}^{n_1} \dots \sum_{j_N=1}^{n_N} A_{j_1 \dots j_N}(t) \varphi_{j_1}^{(1)}(r_1, t) \dots \varphi_{j_N}^{(N)}(r_N, t)\end{aligned}$$

- orthogonal, time-evolving **single particle functions** (spf's) $\varphi_{j_K}^{(K)}(r_K, t)$
- the spf's can be multi-dimensional ("combined modes")
- **configurations** $\Phi_J(r, t) = \prod_{K=1}^N \varphi_{j_K}^{(K)}(r_K, t)$
- obtain time evolution of the **coefficients and spf's** from DF principle

MCTDH – Equations of Motion

Coupled system of coefficient equations and low-dimensional non-linear equations for the spf's:

coefficients:
$$i \frac{dA_J}{dt} = \sum_L \langle \Phi_J | H | \Phi_L \rangle A_L$$

spf's:
$$i \rho^{(\kappa)} \frac{\partial \varphi^{(\kappa)}}{\partial t} = \left(\hat{1} - \hat{P}^{(\kappa)} \right) \hat{H}^{(\kappa)} \varphi^{(\kappa)}$$

- $\rho^{(\kappa)}$ is the reduced density matrix in the κ th subspace
- $\hat{P}^{(\kappa)} = \sum_j |\varphi_j^{(\kappa)}\rangle \langle \varphi_j^{(\kappa)}|$ is the time-dependent projector on the κ th subspace
- $\hat{H}^{(\kappa)}$ is a mean-field Hamiltonian matrix
- simplest case: Time-Dependent Hartree = TDH² (single configuration)

Meyer, Manthe, Cederbaum, CPL **165**, 73 (1990), Beck et al., Phys. Rep. **324**, 1 (2000)

²also denoted Time-Dependent Self-Consistent Field = TDSCF

Scope and Extensions

- MCTDH takes one to 50-100 modes
- exponential scaling ($\sim fN^{f+1}$) not broken but alleviated
- restriction on the form of the potential: sums over products
- related multi-layer variant (ML-MCTDH) goes up to 1000 modes
Wang, Thoss, J. Chem. Phys. 119, 1289 (2003)
- related MCTDH-F (fermion) and MCTDH-B (boson) methods
Kato, Kono, Chem. Phys. Lett. 392, 533 (2004), Nest, Klamroth, Saalfrank, J. Chem. Phys. 122, 124102 (2005)
Alon, Streltsov, Cederbaum, Phys. Lett. A 362, 453 (2007)
- density matrix variant
Raab, Burghardt, Meyer, J. Chem. Phys. 111, 8759 (1999)
- hybrid approaches: e.g., Gaussian-based variant (G-MCTDH, vMCG)
Burghardt, Meyer, Cederbaum, J. Chem. Phys. 111, 2927 (1999), Worth, Burghardt, Chem. Phys. Lett. 368, 502 (2003)

Multi-Layer(ML)-MCTDH: Wavefunction Ansatz

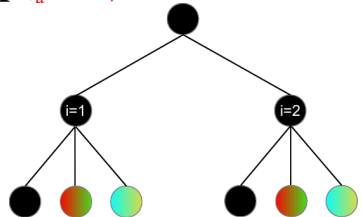
$$\Psi(r, t) = \sum_J A_J(t) \Phi_J(r, t) = \sum_J A_J(t) \prod_{\kappa=1}^M \varphi_{j_\kappa}^{(\kappa)}(r_\kappa, t)$$

where the **1st-layer SPFs** $\varphi_{j_\kappa}^{(\kappa)}$ are now built as superpositions of **2nd-layer SPFs**,

$$\varphi_{j_\kappa}^{(\kappa)}(r_\kappa, t) = \sum_L B_{j_\kappa, L}^{(\kappa)}(t) \Phi_L^{(\kappa)}(r_\kappa, t) = \sum_L B_{j_\kappa, L}^{(\kappa)}(t) \prod_{\mu} \varphi_{l_\mu}^{(\kappa, \mu)}(r_{\kappa\mu}, t)$$

... and so on ...

- intra-SPF correlations *via* MCTDH form
- continue to higher orders: ML-MCTDH
- “hierarchical Tucker format”



Wang, Thoss, J. Chem. Phys. 119, 1289 (2003), Manthe, J. Chem. Phys. 128, 164116 (2008), Vendrell, Meyer, J. Chem. Phys. 134, 044135 (2011)

Multiconfigurational Methods (MCTDH & Co)

**dissipative
modes**

$\{\chi^{(n)}\}$



**primary
modes**

$\{\varphi^{(\kappa)}\}$

**secondary
modes**

$\{g^{(f)}\}$

$$\Psi(r, t) = \sum_J A_J(t) \Phi_J(r, t)$$

$$\text{with } \Phi_J(r, t) = \prod_{\kappa=1}^M \varphi_{j_\kappa}^{(\kappa)}(r_\kappa, t)$$

Multi-Configuration Time-Dependent Hartree

Meyer et al., CPL **165**, 73 (1990), Manthe et al., JCP **97**, 3199 (1992),
Beck et al., Phys. Rep. **324**, 1 (2000)

Multi-layer MCTDH (ML-MCTDH)

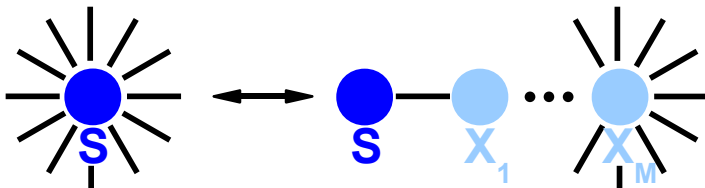
Wang, Thoss, JCP **119**, 1289 (2003), Manthe, JCP **128**, 164116 (2008),
Vendrell, Meyer, JCP **134**, 044135 (2011)

Gaussian variant: (ML-)G-MCTDH & vMCG

$$\Phi_J(r, t) = \underbrace{\prod_{\kappa=1}^M \varphi_{j_\kappa}^{(\kappa)}(r_\kappa, t)}_{\text{primary nodes}} \underbrace{\prod_{\kappa=M+1}^P g_{j_\kappa}^{(\kappa)}(r_\kappa, t)}_{\text{secondary modes}}$$

Burghardt, Meyer, Cederbaum, JCP **111**, 2927 (1999), Burghardt, Giri, Worth,
JCP **129**, 174104 (2008), Römer, Ruckebauer, Burghardt JCP **138**, 064106 (2013)

Reduced-dimensional Models: Collective Modes



Martinazzo, Vacchini, Hughes, Burghardt, J. Chem. Phys. 134, 011101 (2011), Hughes, Christ, Burghardt, J. Chem. Phys. 131, 024109 (2009)
 Tamura, Bittner, Burghardt, J. Chem. Phys. 126, 021103 (2007), Gindensperger, Köppel, Cederbaum, J. Chem. Phys. 126, 034106 (2007)
 Cederbaum, Gindensperger, Burghardt, Phys. Rev. Lett., 94, 113003 (2005), Garg, Onucic, Ambegaokar, J. Chem. Phys. 83, 4491 (1985)

$$\hat{H}_{SB} + \hat{H}_B = \hat{S} \sum_i c_n \hat{x}_n + \hat{H}_B \longrightarrow D \hat{S} \hat{X}_1 + d_{12} \hat{X}_1 \hat{X}_2 + \dots + \hat{X}_M \text{--residual bath}$$

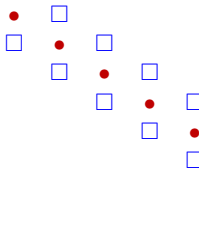
- orthogonal coordinate transformation $\hat{X} = \mathbf{T}\hat{x}$
- short-time dynamics captured by first few effective modes
- truncate the chain – with a (quasi-)Markovian closure – to define an approximate, reduced-dimensional model

Spectral Densities as Continued Fractions

- map spectral densities onto the transformed representation
- “Mori-chain” continued fraction (CF):

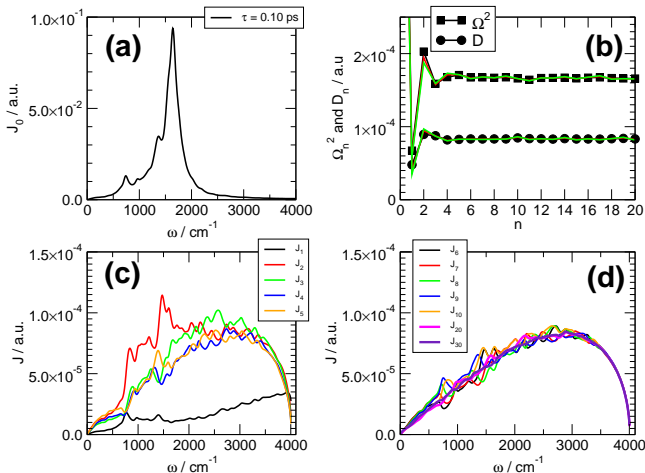
$$J(\omega) = \frac{\pi}{2} \sum_n \frac{c_n^2}{\omega_n} \delta(\omega - \omega_n) \quad \longleftrightarrow \quad J(\omega) = \lim_{\varepsilon \rightarrow 0^+} \operatorname{Im} K(z) \Big|_{z=\omega-i\varepsilon}$$

Hughes, Christ, Burghardt, JCP 131, 024109 (2009), Garg, Onuchic, Ambegaokar, JCP 83, 4491 (1985), Leggett, Phys. Rev. B 30, 1208 (1984)



$$K(z) = - \frac{D^2}{\Omega_1^2 - z^2 - \frac{d_{1,2}^2}{\Omega_2^2 - z^2 - \dots \frac{d_{M-2,M-1}^2}{\Omega_{M-1}^2 - z^2 - \frac{d_{M-1,M}^2}{\Omega_M^2 - z^2 - \dots}}}$$

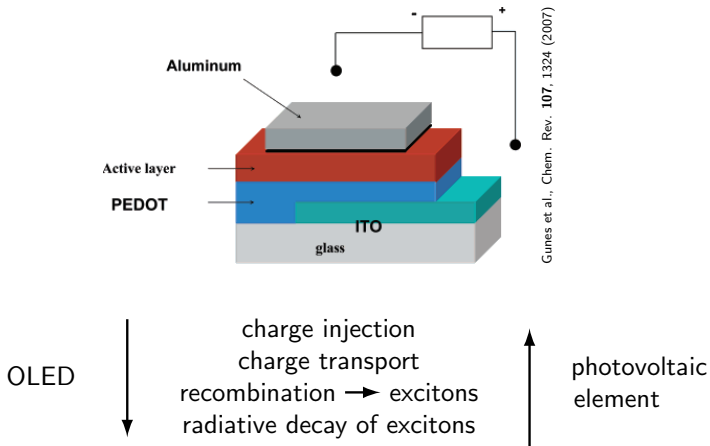
Effective Mode Chains – Convergence to an Ohmic SD



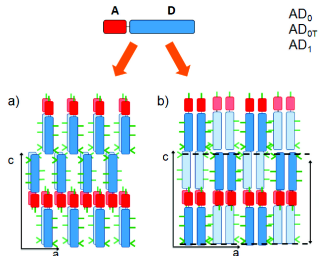
Martinazzo, Vacchini, Hughes, Burghardt, J. Chem. Phys. 134, 011101 (2011)

- residual SD's tend towards a quasi-Ohmic limit (i.e., with cutoff)

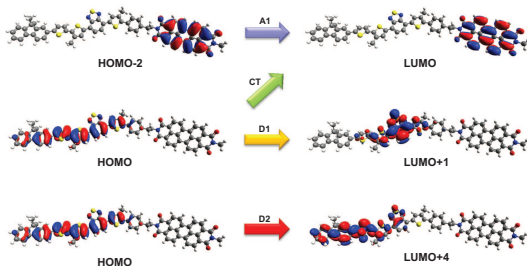
New Materials for Optoelectronics



New Generation of Dyads/Triads



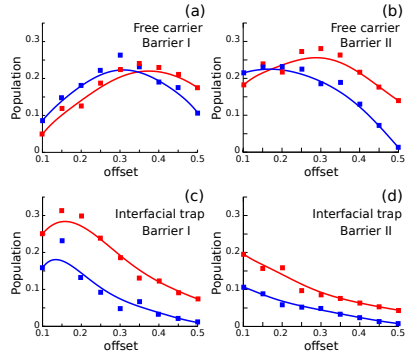
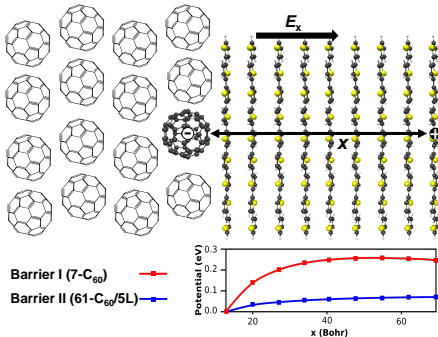
Schwartz et al., JACS 136, 5981 (2014)



Roland, Eisenbrandt et al., in preparation

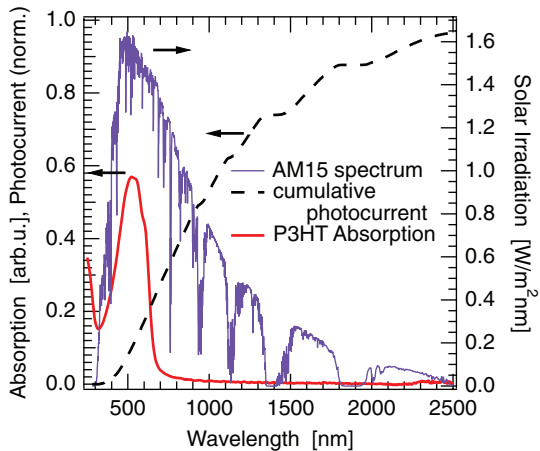
- tunable donor species: alternating thiophene/fluorene/benzothiadiazole units; electrodeficient bridge to the perylene acceptor
- organization in lamellae (both DA and ADA – but not DAD)
- comparatively slow CT formation (hundreds of ps); less recombination

How to Optimize the Free Carrier Yield



- free carrier population \sim IQE (internal quantum efficiency)
- interfacial trap is less populated with increasing offset $\Delta E_{\text{offset}} = \epsilon^{\text{XT}} - \epsilon^{\text{CT}}$
- lower barrier (II) favors free carrier generation

Absorption

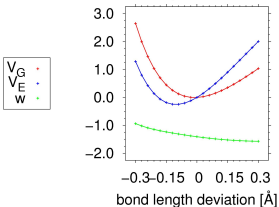
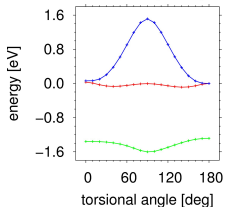
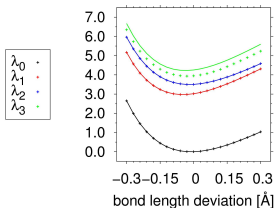
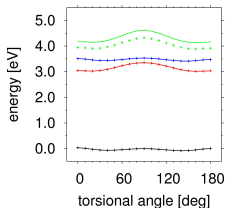


Relevant Coordinates: Torsions + Bond Length Alternation

$$V_{\text{input}} = \begin{pmatrix} * & \dots & * & \lambda_t & * & \dots & * & \lambda_s & * & \dots & * \\ 0 & & & & & & & & & & \lambda_0 \end{pmatrix}$$

↓ Map

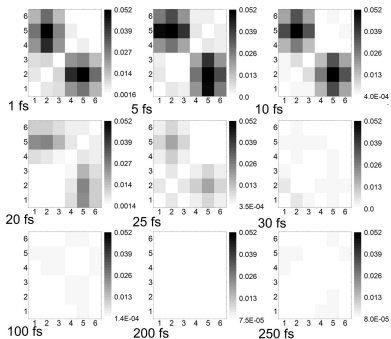
$$= c_G \mathbf{1} + \begin{pmatrix} d & w_0 & & & & & & & & & 0 \\ w_0 & d & w_0 & & & & & & & & \\ & \ddots & \ddots & \ddots & & & & & & & \\ & & w_0 & d & & & & & & & \\ & & & w_0 & d & & & & & & \\ & & & & \begin{matrix} \tilde{d} & w \\ w & \tilde{d} \end{matrix} & w_0 & & & & \\ & & & & w_0 & d & w_0 & & & & \\ & & & & & \ddots & \ddots & \ddots & & & \\ & & & & & & w_0 & d & w_0 & & \\ & & & & & & & w_0 & d & & \\ 0 & & & & & & & & & & d_G \end{pmatrix}$$



- analytical, pointwise mapping of oligomer PES's onto a Frenkel model
- diabatisation in terms of solution to an inverse eigenvalue problem
- applicable to “extended Hückel systems” of J-aggregate or H-aggregate type

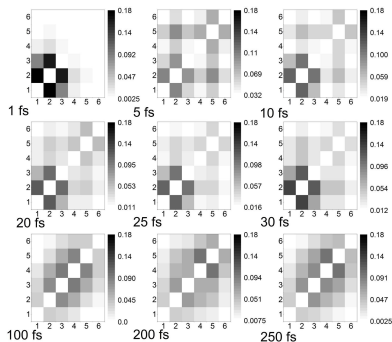
Coherence Evolution

$$\text{Im}\rho_{vv,\mu\mu}(t) = \text{Im}\text{Tr}\{|vv\rangle\langle\mu\mu|\hat{\rho}(t)\}$$



- **Imaginary** part \leftrightarrow population flux
- ultrafast decay time (~ 50 fs)

$$\text{Re}\rho_{vv,\mu\mu}(t) = \text{Re}\text{Tr}\{|vv\rangle\langle\mu\mu|\hat{\rho}(t)\}$$



- **Real** part \leftrightarrow stationary superposition
- reaches stationary LEGS coherence